CALIFORNIA INSTITUTE OF TECHNOLOGY

EARTHQUAKE ENGINEERING RESEARCH LABORATORY

EARTHQUAKE RESPONSE OF TALL REGULAR BUILDINGS

BY

PAUL C. JENNINGS

REPORT NO. EERL 97-01

PASADENA, CALIFORNIA

JANUARY 1997

Tall buildings of downtown Los Angeles, circa 1990

EARTHQUAKE RESPONSE OF TALL REGULAR BUILDINGS

BY

PAUL C. JENNINGS

REPORT NO. EERL 97-01

PASADENA, CALIFORNIA

JANUARY 1997

EARTHQUAKE RESPONSE OF TALL REGULAR BUILDINGS

CHAPTER I--INTRODUCTION

The developments presented in this study of the earthquake response of tall buildings are based on the observation that these structures share many important dynamic properties. Among these are a uniformity with height of cross-sectional area and mass per story, a general similarity in mode shapes of vibration, and similar ratios of higher natural frequencies to those of the fundamental modes.

The study begins by quantifying the similarities and differences in measured mode shapes of tall, regular buildings by expressing them in terms of a common set of basis vectors, a set that is adapted from the mode shapes of a uniform shear beam. The transformation matrix between the mode shapes of a building and the basis vectors contains all the information about the mode shapes, measured against a standard reference. Because the mode shapes of a uniform shear beam are fixed at the base, have the same number of zero crossings as the corresponding modes of tall buildings and the same general shape, the transformation matrix is strongly diagonal.

Quantifying the mode shapes this way and using the simple mathematical form of the basis vectors to evaluate some key expressions allows the development of simplified, general formulas for important measures of earthquake response of tall buildings as a class of structures. Relations are developed for maximum modal values of base shear, base moment, drift at the first floor level, and for displacement and acceleration on the roof. These modal maxima depend upon mode number, j, the modal period, the pseudo-velocity response spectrum ordinate, and upon one or two parameters of the mode shape. The parameters of the mode shape are taken from a set of four which are each simple summations calculated from the elements of the j^{th} column of the transformation matrix.

The next step in the study was to use data from ambient and forced vibration tests of building to determine numerical values for the elements and parameters of the transformation matrices. The general similarity in mode shapes of tall, regular buildings encourages the expectation that the ranges of important parameters will be sufficiently small that useful averages and trends can be identified. Data from tests of eleven tall buildings, nearly all tested in both horizontal directions, allowed

meaningful calculations to be made for the first five modes of vibration. The four modal parameters were found to be well-defined for the lower modes of vibration, with only moderate levels of variation. The average parameters for the especially important fundamental mode are particularly well-defined, showing a standard deviation of ten percent or less.

The average values and standard deviations of the four mode shape parameters were then introduced into the relations giving modal maxima of measures of earthquake response. Also introduced were average values of the period ratios for the tall buildings, determined from the set of experiments mentioned above, and assumptions regarding the general shape of the pseudo-velocity response spectrum. Modal values were then combined by the method of the square root of the sum of the squares. The resulting simple formulas for average values of the base shear, base moment, first floor drift, and roof displacement and acceleration of tall buildings depend only on the response spectrum ordinate and the period of the fundamental mode of vibration, and in the case of the first floor drift, upon the height of the building. The variation in the results attributable to variations in structural mode shapes and periods was approximated and appears to be much less than that inherent in determining the appropriate level of the response spectrum. An example gives values for a representative building with a five second fundamental period subjected to the general level of motion experienced in the northern San Fernando Valley during the Northridge earthquake.

The approach of this study is directly applicable to the low levels of motion of typical vibration tests; for moderate earthquake motions the fundamental period and the level of damping should be values appropriate to the expected level of response. For the most important case, that of the response of tall buildings to strong earthquake motion, the results are applicable if one makes the assumption that successful response, although non-linear, is describable by linear models with appropriate periods and equivalent dampings. In other words, that structural yielding and non-structural damage are not excessive and are well-distributed over the structure. The results are not applicable if the damage becomes highly concentrated or if failure occurs.

The results presented below are believed to useful in assessing the potential earthquake response of tall buildings when the detailed properties of the structures are not known. The buildings could be examined individually, or as a group as part of an analysis of urban earthquake hazard. The results are also believed applicable to the determination of seismic design criteria and to the related problem of estimating the

demands placed on existing structures by strong ground motion, e. g., the levels of base shear, base moment, etc. that must be met if the damage is to be limited to levels describable by equivalent linear response. The approach is not intended to replace the calculation of response to specific ground motions that is often done in the final stages of the design of a tall building.

The next two chapters are devoted to the presentation of the analysis and to the introduction of response spectrum methods into the approach. They are followed by a chapter which applies the analysis to data from vibration tests of tall buildings and consolidates the resulting information. Chapter five uses the results of previous chapters to develop simple expressions for selected measures of earthquake response. The final chapter contains conclusions and discussion of the results and underlying assumptions. The report concludes with references and appendices, one containing notes on the data reduction and another giving the transformation matrices determined from test data.

CHAPTER II--ANALYSIS

Equations of Motion

The analysis considers the planar vibrations of a tall, n-story building with equal floor masses, m; the mass matrix, **M**, is proportional to the identity matrix. The total mass of the structure is m_0, and the height is l. The stiffness matrix, **K**, is positive definite, real and symmetric, but is otherwise arbitrary. The damping matrix, **C**, is assumed to be such that the structure possesses classical normal modes to an acceptable approximation. The horizontal direction is denoted by x, and the vertical direction by y. Deflections in the x-direction with respect to the base are expressed as u_i, in which i, the floor level, varies from 1 to n. The horizontal acceleration at the base of the structure is given by $\ddot{u}_g$. The notation is illustrated in Figure 1.

Under these conditions, the equation of motion can be written as

$$\mathbf{M}\underline{\ddot{u}} + \mathbf{C}\underline{\dot{u}} + \mathbf{K}\underline{u} = -\mathbf{M}\,\underline{1}\,\ddot{u}_g(t). \tag{1}$$

Premultiplying by the inverse of the mass matrix gives

$$\mathbf{I}\underline{\ddot{u}} + \mathbf{M}^{-1}\mathbf{C}\underline{\dot{u}} + \mathbf{M}^{-1}\mathbf{K}\underline{u} = -\underline{1}\,\ddot{u}_g(t). \tag{2}$$

Let $\underline{\phi_j}$, $j = 1, \ldots, n$, be the modes of the undamped eigenvalue problem

$$\mathbf{I}\underline{\ddot{u}} + \mathbf{M}^{-1}\mathbf{K}\underline{u} = 0, \tag{3}$$

normalized so that the modal matrix, Φ, is orthonormal, i. e.,

$$\underline{\phi_i}^T\underline{\phi_j} = \delta_{ij} \quad , \quad i, j = 1, \ldots, n. \tag{4}$$

To transform the equations of motion to normal coordinates, let

$$\underline{u} = \Phi\underline{\xi}. \tag{5}$$

Substituting into Eqn. 2, premultiplying by Φ^T, and using the properties of Φ and those assumed for **C** produces the uncoupled set of equations

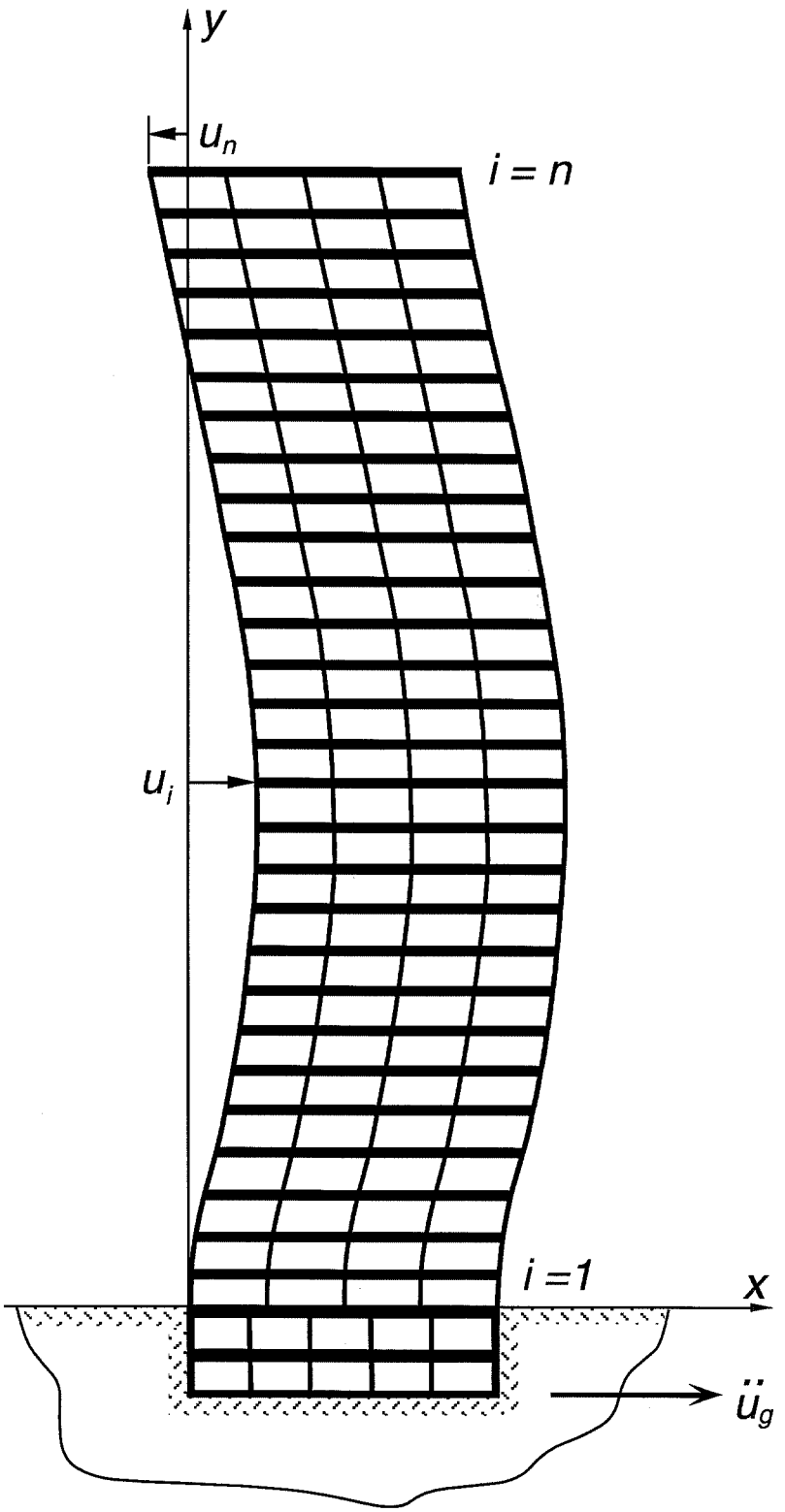

Figure 1. Response of a tall regular building to earthquake motion

$$\mathbf{I}\underline{\ddot{\xi}} + \tilde{\mathbf{C}}\underline{\dot{\xi}} + \Omega^2\,\underline{\xi} = -\Phi^T\,\underline{1}\,\ddot{u}_g(t), \tag{6}$$

in which the matrices $\tilde{\mathbf{C}} = [2\omega_j\,\zeta_j]$ and $\Omega^2 = [\omega_j^2]$ are diagonal. The natural frequency and damping of the j^{th} mode are given by ω_j and ζ_j, respectively.

From Eqn. 6, the equation of motion of the j^{th} mode can be written as

$$\ddot{\xi}_j + 2\omega_j\,\zeta_j\,\dot{\xi}_j + \omega_j^2\,\xi = -\alpha_j\,\ddot{u}_g(t), \tag{7}$$

with the modal participation factor, α_j, given by

$$\alpha_j = \underline{\phi_j^T}\,\underline{1}\,. \tag{8}$$

The modal participation factor defined by Eqn. 8 has the limitation noted by Chopra (1996) that it is dependent on the way the modes have been normalized by Eqn. 4. However, it is convenient for the present analysis that the modes be orthonormal. If Eqn. 8 is expanded,

$$\alpha_j = \{\phi_{1j},\ \ \phi_{2j},\ \ \ldots,\ \ \phi_{nj}\}\begin{Bmatrix}1\\1\\\vdots\\1\end{Bmatrix} = \sum_{i=1}^{n}\phi_{ij}\,, \tag{9}$$

it is seen that in this form the participation factor is given by the sum of the modal coordinates. For modes greater than the first, the modal coordinates will be both positive and negative and α_j can be interpreted as the geometrical imbalance of the mode shape; a mode with equal positive and negative components will not be excited by base excitation.

Basis Vectors

Any motion of the structure can be expressed as a sum of responses of the normal modes, $\underline{\phi_j}$, $j = 1, \ldots, n$. In mathematical terms, the modes form a vector space of dimension n which spans the range of possible displacements of the structure. However, other sets of vectors can also span this space. Consider an n-dimensional square matrix of such vectors

$$\Psi = \left[\underline{\psi_1},\ \underline{\psi_2},\ \ldots,\ \underline{\psi_n}\right] = \left[\psi_{ij}\right]. \tag{10}$$

The column vectors of the matrix Ψ also form a basis for the space spanned by the modes $\underline{\phi_j}$ and, hence, for the displacement of the structure. Like the modal matrix, Φ, Ψ is chosen to be orthonormal.

In this study, the columns of Ψ are vectors based on the modes of a uniform, continuous shear beam. The shear beam modes were chosen because they are simple in form, allowing the evaluation of certain key expressions, and because they are geometrically similar in form to the measured mode shapes of tall regular buildings. These properties of the modes of a uniform shear beam are well-known and the shear beam is often used in earthquake response studies (e.g., Biot, 1932; Rosenblueth, 1951; Jennings, 1959; Newmark and Rosenblueth, 1971; Iwan, 1996).

The analysis proceeds by expanding the modes, $\underline{\phi_j}$, in terms of the basis vectors, $\underline{\psi_j}$.

$$\underline{\phi_j} = b_{1j}\underline{\psi_1} + b_{2j}\underline{\psi_2} + \cdots + b_{nj}\underline{\psi_n} = \left[\underline{\psi_1},\ \underline{\psi_2},\ \ldots,\ \underline{\psi_n}\right]\begin{Bmatrix} b_{1j} \\ b_{2j} \\ \vdots \\ b_{nj} \end{Bmatrix},\ j = 1,\cdots,n. \tag{11}$$

Combining into matrix form,

$$\begin{bmatrix} \phi_{11} & \phi_{12} & \cdots & \phi_{1n} \\ \phi_{21} & \phi_{22} & \cdots & \phi_{2n} \\ \vdots & \vdots & \ddots & \vdots \\ \phi_{n1} & \phi_{n2} & \cdots & \phi_{nn} \end{bmatrix} = \begin{bmatrix} \psi_{11} & \psi_{12} & \cdots & \psi_{1n} \\ \psi_{21} & \psi_{22} & \cdots & \psi_{2n} \\ \vdots & \vdots & \ddots & \vdots \\ \psi_{n1} & \psi_{n2} & \cdots & \psi_{nn} \end{bmatrix}\begin{bmatrix} b_{11} & b_{12} & \cdots & b_{1n} \\ b_{21} & b_{22} & \cdots & b_{2n} \\ \vdots & \vdots & \ddots & \vdots \\ b_{n1} & b_{n2} & \cdots & b_{nn} \end{bmatrix}, \tag{12}$$

or

$$\Phi = \Psi\mathbf{B}. \tag{13}$$

Equation 12 or 13 defines the transformation matrix, $\mathbf{B}$. Because both Φ and Ψ are orthonormal, so is $\mathbf{B}$. Premultiplying Eqn. 13 by $\Psi^{\mathrm{T}} = \Psi^{-1}$ yields

$$\mathbf{B} = \Psi^{T}\Phi. \tag{14}$$

Equation 14 states that the transformation matrix, **B**, can be found from the measured mode shapes of the tall building under study. Test results from several buildings are examined in the next chapter to determine the properties of **B**.

Since the modes of a uniform shear beam are geometrically quite similar to the measured modes of tall structures, it is expected that **B** will be strongly diagonal, i.e.,

$$\mathbf{B} = \mathbf{I} + \mathbf{E}, \tag{15}$$

in which $\mathbf{E} = [e_{ij}]$ has terms generally less than unity. The defining equations ensure that the transformation matrix, **B**, will approach the identity matrix as the structural mode shapes approach those of a uniform shear beam.

Shear Beam Modes

The mode shapes of a continuous, uniform shear beam can be written as

$$\psi_j(y) = \gamma(-1)^{j+1} \sin\frac{(2j-1)\pi y}{2l}, \tag{16}$$

in which γ is a normalization factor, independent of j in the case of a continuous and uniform shear beam. Because it is the integrated properties of the continuous mode shapes that are convenient to preserve when constructing the discrete modes, the discrete versions of the shear beam modes are determined from an analysis of areas. For a continuous function of y, $f(y)$, and with n large.

$$\sum_{i=1}^{n} \Delta y\, f\left(y_i - \frac{\Delta y}{2}\right) \approx \int_0^l f(y)\,dy, \tag{17}$$

in which y_i is the height of the i^{th} level and $\Delta y = \frac{l}{n}$ is the distance between levels. Letting $f(y)$ in Eqn. 17 be the square of the mode shape of Eqn.

16, and recalling that the vectors $\underline{\psi_j}$ are to form an orthonormal set, leads to the following discrete version of the shear beam mode shapes

$$\underline{\psi_j} = (-1)^{j+1}\sqrt{\frac{2}{n}}\sin\frac{(2j-1)\pi}{2}\left(\frac{y_i}{l}-\frac{1}{2n}\right) \qquad i,j=1,\ldots,n. \tag{18}$$

Although developed through the approximation of Eqn. 17, the set of n vectors in Eqn. 18 are, in this case, exactly orthonormal.

Participation Factors

The next step is to introduce the transformation **B** into the expression for the participation factors. Because a scalar is equal to its transpose, Eqn. 8 can also be written

$$\alpha_j = \{1,\ 1,\ \cdots,\ 1\}\,\underline{\phi_j}. \tag{19}$$

Substituting from Eqn. 11 gives

$$\alpha_j = \{1,\ 1,\ \cdots,\ 1\}\begin{bmatrix}\psi_{11} & \psi_{12} & \cdots & \psi_{1n}\\ \psi_{21} & \psi_{22} & \cdots & \psi_{2n}\\ \vdots & \vdots & \ddots & \vdots\\ \psi_{n1} & \psi_{n2} & \cdots & \psi_{nn}\end{bmatrix}\begin{Bmatrix}b_{1j}\\ b_{2j}\\ \vdots\\ b_{nj}\end{Bmatrix}. \tag{20}$$

Evaluating Eqn. 20 conveniently from the left yields

$$\alpha_j = b_{1j}\sum_{i=1}^{n}\psi_{i1} + b_{2j}\sum_{i=1}^{n}\psi_{i2} + \cdots + b_{nj}\sum_{i=1}^{n}\psi_{in}. \tag{21}$$

The simple mathematical form of the shear beam modes, $\underline{\psi_j}$, allows the summations in Eqn. 21 to be evaluated. Applying Eqn. 17 to the modes $\underline{\psi_j}$ given by Eqn. 18 produces

$$\sum_{i=1}^{n}\psi_{ij}\left(y_i-\frac{\Delta y}{2}\right) \approx \frac{1}{\Delta y}\int_0^l \psi_j(y)\,dy. \tag{22}$$

Substituting from Eqn. 16, with $\gamma = \sqrt{\frac{2}{n}}$, and evaluating the integral in Eqn. 22 gives

$$\sum_{i=1}^{n} \psi_{ij} \approx \frac{(-1)^{j+1}\, 2\sqrt{2n}}{(2j-1)\,\pi}, \tag{23}$$

which is a very close approximation for n large. Assuming equality in Eqn. 23 and substituting into Eqn. 21 gives the following expression for the participation factors

$$\alpha_j = \frac{2\sqrt{2n}}{\pi(2j-1)}\, p_j \qquad j = 1, \cdots, n, \tag{24}$$

in which

$$p_j = (2j-1)\left[b_{1j} - \frac{b_{2j}}{3} + \frac{b_{3j}}{5} - \frac{b_{4j}}{7} + \cdots + \frac{(-1)^{n+1}\, b_{nj}}{(2n-1)} \right]. \tag{25}$$

The participation factors, α_j, are seen to depend on the mode number, j, the number of stories, n, (a feature of the normalization method), and the factor p_j, which is a weighted sum of the elements of the j^{th} column of the transformation matrix, **B**. As the modes of the structure approach those of the uniform shear beam, **B** approaches the identity matrix and p_j approaches unity. However, it is important to appreciate that Eqns. 24 and 25 are valid in the general case, even if the structural modes differ significantly from those of the uniform shear beam.

CHAPTER III--APPLICATION OF RESPONSE SPECTRUM METHODS

Earthquake response spectra are defined by the maximum absolute value of a selected response parameter of a simple oscillator. Spectra are formed by plotting the maximum value of the response, typically displacement, velocity or acceleration, as a function of the oscillator's fraction of critical damping, ζ, and its circular natural frequency, ω, or period, $T = \frac{2\pi}{\omega}$. In this study, the commonly used pseudo-velocity spectrum is employed (Housner, 1970; Chopra, 1995). The pseudo-velocity is defined by ω times the maximum oscillator displacement and will denoted herein by $S_{pv}(T,\zeta)$.

The modal equation, Eqn. 7, is the same as the defining equation for the response spectra of the earthquake motion, $\ddot{u}_g$, except for the multiplicative factor, α_j. The maximum value of ξ_j can therefore be written as

$$\xi_j(\max) = \frac{\alpha_j T_j}{2\pi} S_{pv}(T_j,\zeta_j). \tag{26}$$

Returning to physical coordinates via Eqn. 6, and substituting for α_j from Eqn. 24,

$$\underline{u_j}(\max) = \xi_j(\max)\,\underline{\phi_j} = \frac{\sqrt{2n}\,T_j}{\pi^2(2j-1)} S_{pv}(T_j,\zeta_j)\,p_j\,\underline{\phi_j}. \tag{27}$$

Applying Eqn. 11,

$$\underline{u_j}(\max) = \frac{\sqrt{2n}\,T_j}{\pi^2(2j-1)} S_{pv}(T_j,\zeta_j)\,p_j \begin{bmatrix} \psi_{11} & \psi_{21} & \cdots & \psi_{1n} \\ \psi_{21} & \psi_{22} & \cdots & \psi_{2n} \\ \vdots & \vdots & \ddots & \vdots \\ \psi_{n1} & \psi_{n2} & \cdots & \psi_{nn} \end{bmatrix} \begin{Bmatrix} b_{1j} \\ b_{2j} \\ \vdots \\ b_{nj} \end{Bmatrix}. \tag{28}$$

An alternate form of Eqn. 28 is obtained by using Eqn. 18,

$$\underline{u_j}(\max) = \frac{2\,T_j}{\pi^2(2j-1)} S_{pv}(T_j,\zeta_j)\, p_j \left[(-1)^{j+1} \sin\frac{(2j-1)\pi}{2}\left(\frac{y_i}{l} - \frac{1}{2n}\right)\right] \begin{Bmatrix} b_{1j} \\ b_{2j} \\ \vdots \\ b_{nj} \end{Bmatrix} \qquad (29)$$

$i, j = 1, \cdots, n.$

Equations 28 and 29 (note that n no longer appears) express the maximum displacement of the j^{th} mode of the structure at each level i as a function of the response spectrum of the ground motion, the basis vectors, and the elements of the j^{th} column of the matrix **B**. Because of the nature of $S_{pv}(T,\zeta)$, factors that multiply it, including α_j, p_j, etc., can be taken as positive without loss of generality.

Important measures of earthquake response of tall buildings can be evaluated from these equations for $\underline{u_j}(\max)$ following, in general terms, an approach of a previous study (Jennings 1969).

Displacement at the Roof of the Structure

The displacement at the roof of the structure is an easily understood and communicated parameter of earthquake response. Although it is not often as directly useful to engineers as parameters such as base shear and interstory drift, it does have the advantage of being readily understood by the general public. Equation 28 or 29 can be used to determine the modal displacement of the structure at the roof. The matrix elements on the bottom row ($i = n$; $y_i = l$) of Eqn. 28 are given by

$$\psi_{nj} = \sqrt{\frac{2}{n}} \cos\frac{(2j-1)\pi}{4n} \qquad j = 1, \cdots, n. \qquad (30)$$

Equation 30 allows u_{nj}, the j^{th} modal component of the displacement at the roof of the structure, to be calculated by performing the matrix multiplication in Eqn. 28 for the bottom row. This can be done with sufficient accuracy for most purposes using the fact that the cosine function in Eqn. 30 is very close to unity for small j. For example, if the maximum mode number of interest is one-sixth the number of stories, the following formula has a maximum overestimation error of less than 5 per cent; for modes up to one-fourth the number of stories, the overestimation is less than 8 per cent.

$$u_{nj}(\max) \approx \frac{2T_j}{\pi^2(2j-1)} S_{pv}(T_j, \zeta_j) p_j \, q_j. \tag{31}$$

In Eqn. 31

$$q_j = \sum_{i=1}^{n} b_{ij} \tag{32}$$

is the sum of the elements of the j^{th} column of the transformation matrix. Note that q_j, like p_j, approaches unity as the structural modes approach those of a uniform shear beam.

Base Shear

Using the present notation, the maximum base shear, V_j, generated by the j^{th} mode of earthquake response can be written, in general, as

$$V_j(\max) = \alpha_j^2 \frac{2\pi}{T_j} S_{pv}(T_j, \zeta_j) \underline{\phi_j^T} \mathbf{M} \underline{\phi_j}. \tag{33}$$

Substituting for α_j and using the properties of $\mathbf{M}$ and the mode shapes, $\underline{\phi_j}$,

$$V_j(\max) = \frac{16 m_0}{\pi(2j-1)^2 T_j} S_{pv}(T_j, \zeta_j) p_j^2. \tag{34}$$

The base shear is often expressed as a fraction of the total weight, $m_0 g$, of the structure, in which g is the acceleration of gravity. From Eqn. 34, this fraction is

$$\frac{V_j}{m_0 g}(\max) = \frac{16}{\pi g(2j-1)^2 T_j} S_{pv}(T_j, \zeta_j) p_j^2. \tag{35}$$

Interstory Drift

Interstory deflections of buildings are termed drifts and are usually expressed as the ratio of the interstory deflection to the interstory height. The drift ratio defines an angle which is, in essence, the discrete version of the partial derivative of the displacement with respect to height. This

relation has been used by W. D. Iwan (1996) to define drift spectra of strong ground motion.

Employing this approach, the drift ratio for displacement in the j^{th} mode can be approximated from Eqn. 27 by

$$\underline{d_j}(\max) = \frac{\sqrt{2n}\,T_j}{\pi^2(2j-1)} S_{pv}\left(T_j,\zeta_j\right) p_j \left.\frac{\partial \phi_j}{\partial y}\right|_{y=y_i} . \tag{36}$$

Substituting from Eqn. 11, and letting $\psi'_{ij} = \left.\frac{\partial \psi_j}{\partial y}\right|_{y=y_i}$,

$$\underline{d_j}(\max) = \frac{\sqrt{2n}\,T_j}{\pi^2(2j-1)} S_{pv}\left(T_j,\zeta_j\right) p_j \begin{bmatrix} \psi'_{11} & \psi'_{21} & \cdots & \psi'_{1n} \\ \psi'_{21} & \psi'_{22} & \cdots & \psi'_{2n} \\ \vdots & \vdots & \ddots & \vdots \\ \psi'_{n1} & \psi'_{n2} & \cdots & \psi'_{nn} \end{bmatrix} \begin{Bmatrix} b_{1j} \\ b_{2j} \\ \vdots \\ b_{nj} \end{Bmatrix}. \tag{37}$$

Using Eqn. 18 to evaluate ψ'_{ij} gives

$$\underline{d_j}(\max) = \frac{T_j}{\pi l} S_{pv}\left(T_j,\zeta_j\right) p_j \left[(-1)^{j+1} \cos\frac{(2j-1)\pi}{2}\left(\frac{y_i}{l} - \frac{1}{2n}\right)\right] \begin{Bmatrix} b_{1j} \\ b_{2j} \\ \vdots \\ b_{nj} \end{Bmatrix}, \tag{38}$$

$i, j, = 1, \cdots, n.$

The modal drift at the base of the structure ($i = 1;\ y_i = \Delta y$) can be determined from Eqn. 38 by carrying out the indicated matrix multiplication for the top row, using the result that for $i = 1$,

$$(-1)^{j+1} \cos\frac{(2j-1)\pi}{2}\left(\frac{y_i}{l} - \frac{1}{2n}\right)\Bigg|_{i=1} = (-1)^{j+1} \cos\frac{(2j-1)\pi}{4n}. \tag{39}$$

However, as was the case for the modal displacement at the roof of the structure, advantage can be taken of the fact that the cosine function on the right side of Eqn. 39 is close to unity for small j Thus, for the first several modes

$$d_{1j}(\max) \approx \frac{T_j}{\pi l} S_{pv}(T_j, \zeta_j) p_j r_j, \tag{40}$$

in which

$$r_j = \sum_{i=1}^{n} (-1)^{i+1} b_{ij} \tag{41}$$

is the sum of the elements of the j^{th} column of the transformation matrix multiplied by $(-1)^{i+1}$. The algebraic signs inside the summation are relevant, but r_j itself may be taken as positive. Like p_j and q_j, r_j approaches unity as the structural modes approach those of a uniform shear beam.

Base Moment

In general, the maximum moment at the base of the structure, H_j, caused by motions in the j^{th} mode can be expressed as

$$H_j(\max) = \frac{2\pi \alpha_j}{T_j} S_{pv}(T_j, \zeta_j) \underline{\phi}_j^T \mathbf{M} \underline{h}, \tag{42}$$

wherein

$$\underline{h} = \begin{Bmatrix} y_1 \\ y_2 \\ \vdots \\ y_n \end{Bmatrix}. \tag{43}$$

Substituting from Eqn. 24 and using the properties of $\mathbf{M}$ and $\underline{\phi}_j$, Eqn. 42 becomes

$$H_j(\max) = \frac{4m\sqrt{2n}}{T_j(2j-1)} S_{pv}(T_j, \zeta_j) p_j \underline{\phi}_j^T \underline{h}. \tag{44}$$

Because $\underline{\phi}_j^T \underline{h}$ is a scalar, one can write with the help of Eqn. 11

$$\underline{\phi_j^T}\,\underline{h} = \underline{h}^T\,\underline{\phi_j} = \{y_1 \quad y_2 \quad \cdots \quad y_n\}\begin{bmatrix} \psi_{11} & \psi_{21} & \cdots & \psi_{1n} \\ \psi_{21} & \psi_{22} & \cdots & \psi_{2n} \\ \vdots & \vdots & \ddots & \vdots \\ \psi_{n1} & \psi_{n2} & \cdots & \psi_{nn} \end{bmatrix}\begin{Bmatrix} b_{1j} \\ b_{2j} \\ \vdots \\ b_{nj} \end{Bmatrix}. \tag{45}$$

The general, k^{th}, term in the transposed vector produced by $\underline{h}^T\Psi$ is

$$\sum_{i=1}^{n} y_i\,\psi_{ik}. \tag{46}$$

Applying Eqn. 17,

$$\sum_{i=1}^{n} y_i\,\psi_{ik} \approx \frac{n}{l}\int_0^l y\,\underline{\psi_k}(y)\,dy. \tag{47}$$

Using Eqn. 18 to evaluate the integral and assuming equality for large n yields

$$\sum_{i=1}^{n} y_i\,\psi_{ik} = \frac{4l\sqrt{2n}}{(2k-1)^2\pi^2} \tag{48}$$

for the k^{th} term of $\underline{h}^T\Psi$. Substituting into Eqn. 45, collecting terms, and normalizing conveniently by dividing by $m_0 g l$,

$$\frac{H_j}{m_0 g l}(\max) = \frac{32}{\pi^2 g (2j-1)^3 T_j} S_{pv}\left(T_j, \zeta_j\right) p_j s_j, \tag{49}$$

the new parameter, s_j is given by

$$s_j = (2j-1)^2\left[b_{1j} + \frac{b_{2j}}{9} + \frac{b_{3j}}{25} + \frac{b_{4j}}{49} + \cdots + \frac{b_{nj}}{(2n-1)^2}\right]. \tag{50}$$

Again, the parameter s_j is such that it approaches unity as the structural modes approach those of a uniform shear beam. However, for j large the multiplication and division by large numbers makes s_j ill-conditioned and it is convenient to introduce

$$s_j' = \frac{s_j}{(2j-1)^2} \tag{51}$$

and to replace Eqn. 49 by

$$\frac{H_j}{m_0 g l}(\max) = \frac{32}{\pi^2 g (2j-1) T_j} S_{pv}(T_j, \zeta_j)\, p_j s'_j. \tag{52}$$

Note that for $j = 1$, $s'_j = s_j$.

Roof Acceleration

The maximum value of the j^{th} modal component of the total acceleration of the structure can be expressed, in general, as

$$\underline{a_j}(\max) = \frac{2\pi \alpha_j}{T_j} S_{pv}(T_j, \zeta_j)\, \underline{\phi_j}. \tag{53}$$

Substituting from Eqn. 11 and from Eqn. 24,

$$\underline{a_j}(\max) = \frac{4\sqrt{2n}}{(2j-1)T_j} S_{pv}(T_j, \zeta_j) p_j \begin{bmatrix} \psi_{11} & \psi_{21} & \cdots & \psi_{1n} \\ \psi_{21} & \psi_{22} & \cdots & \psi_{2n} \\ \vdots & \vdots & \ddots & \vdots \\ \psi_{n1} & \psi_{n2} & \cdots & \psi_{nn} \end{bmatrix} \begin{Bmatrix} b_{1j} \\ b_{2j} \\ \vdots \\ b_{nj} \end{Bmatrix}. \tag{54}$$

Eqn. 54 is similar to Eqn. 28, and an alternate form if needed, similar to Eqn. 29, can be generated by applying Eqn. 18.

The acceleration at the roof of the structure is of particular interest because of the mechanical equipment that is typically installed there. For $i = n$, the matrix elements on the bottom row of Eqn. 54 are given by Eqn. 30, which allows $a_{nj}(\max)$ to be calculated. However, following the development of Eqn. 31, the first several modes, $a_{nj}(\max)$ are approximated closely by

$$a_{nj}(\max) \approx \frac{8}{(2j-1)T_j} S_{pv}(T_j, \zeta_j) p_j q_j. \tag{55}$$

The foregoing analysis shows that response spectrum methods can be used to express the maximum response of the structure in the j^{th} mode in

terms of structural parameters, the shear beam basis vectors, and properties of the j^{th} column of the transformation matrix, **B**. In particular, simple expressions for the important modal quantities of roof displacement, base shear, base moment, first story drift and roof acceleration have been given. The effect of the mode shapes on these response quantities is embodied in the four parameters p_j, q_j, r_j, and s_j or s'_j, all of which approach unity [or $1/(2j-1)^2$ in the case of s'_j] as the modes of the tall building approach those of a uniform shear beam. The next chapter is devoted to determining ranges of these parameters from experimental data.

CHAPTER IV--DATA FROM BUILDING TESTS

Introduction

The matrix **B** can found by evaluating Eqn. 14, using shear beam basis vectors, $\underline{\psi_j}$, of the appropriate number and dimension, and measured mode shapes, $\underline{\phi_j}$, from vibration tests of tall buildings. However, the calculation of **B** is limited by the fact that in every case only a few, lower modes of vibration have been determined experimentally. Another less important limitation of most tests is that data are rarely taken at every floor level.

Characteristics of the Test Data

Detailed measurements of mode shapes have been acquired two ways. In ambient tests, the response of the structure to wind and traffic excitation is measured with instruments sensitive enough to measure these motions, which are typically below the level of human perception. Statistical methods, for example, Fourier spectrum analysis or system identification techniques are then used to determine the resonant frequencies and mode shapes. This method is limited by unsteady behavior of the excitation and uncertainties in its source. Forced vibration methods of testing use eccentric mass vibrators with precise frequency control to subject the building to harmonic forces. Resonant frequencies are found and the response of the structure at resonance is used to determine the associated mode shape. This method is limited at low frequencies by the magnitude of the exciting force, which is proportional to the frequency squared, and at high frequencies by mechanical stresses in the vibrator and the difficulty of controlling the frequency of excitation. Unless system identification techniques are employed, both methods can be limited by the fact that the response at the resonant frequency of a given mode also contains off-resonant response of other modes.

A compilation of mode shapes and natural frequencies from 39 ambient and forced vibration tests of buildings was assembled by Paul Burridge and Armineh Nalbandian (1983). From this compilation, eleven buildings were judged to meet the criteria of being tall, regular buildings of modern construction. The buildings are in the United States, Japan and Canada. All are steel frame construction, all are designed to resist earthquake motions, and all but two are moment resistant frames. The nominal number of stories varies from 10 to 44. Although Burridge and

Nalbandian's compilation was completed over ten years ago, it appears to include most of the relevant data.

In reporting their experiments, most researchers have presented their measured mode shapes to two significant figures, with the mode normalized to a value of unity at the roof level. Occasionally, the modal ordinates exceed unity; in these cases three significant figures are used. This general level of precision is used in data reduction for this study.

The methods of this study require the measured mode shape, $\underline{\phi_j}$, to be defined at equally-spaced intervals and assumes that the ordinate is zero at $y=0$. Because tall buildings often rise from a few stories of parking structure or some other broad base of a different dimension and structural type, or have basements and sub-basements below grade level, each case was examined individually to determine the most appropriate level to take as the base level, $y=0$.

Most tall buildings have equally-spaced floor levels throughout their height, except at the base, where one or two story heights are often greater, and at the top where the roof sometimes has a different interstory height. In some tests, certain floors could not be occupied for measurement, causing a gap in the measured mode shape. These situations were handled on a case-by-case basis. Missing data were linearly interpolated from the data above and below missing levels; linear interpolation was also used to produce equally-spaced modal ordinates at the base of some structures. In some experiments, modal ordinates were measured at levels within $y/l=0.02$ (in one case 0.03) of regular spacing In these cases the measured modal ordinate was assumed to hold for the corresponding regularly-spaced level. Appendix I gives brief notes describing the steps needed in each case to reduce the data to a specific number of equally-spaced levels. The levels typically correspond to the nominal interstory height of the building, or multiples of that height.

The resulting data set is significant, particularly for lower modes of response, but it is obviously small and rather heterogeneous. Also, it is noted that although most floor masses of the structures are essentially the same, the existence of floors devoted to mechanical equipment and floors with different functions than the rest of the building imply that the story masses of the buildings are not truly identical. These limitations may contribute scatter to the data, but do not seem so serious as to obscure important characteristics in the results.

Determining the Number of Basis Vectors

Equations 11 through 14 show that the calculation of **B** develops via the composition of a measured mode, $\underline{\phi_j}$, from a linear combination of the basis vectors, $\underline{\psi_j}$. Because the number of zero crossings in $\underline{\phi_j}$ is the same as in $\underline{\psi_j}$, and because they are generally similar, the largest contribution by far to the composition of $\underline{\phi_j}$ comes from $\underline{\psi_j}$. Additional contributions, which can be viewed as corrections to this major first approximation, typically come from vectors with numbers near j, some corrections come from lower numbered vectors and some from higher number ones.

If all the basis vectors are used in the linear combinations, each of the measured modes, $\underline{\phi_j}$, can be recomposed exactly. The difficulty in this straightforward approach is that at some stage using more basis vectors reduces to fitting error and noise in the measured mode shapes, and thereby introduces error into the analysis. Therefore, the number of basis vectors was limited, as described below.

Expanding Eqn. 14,

$$\mathbf{B} = \Psi^{\mathrm{T}}\Phi = \begin{bmatrix} \underline{\psi_1^T} \\ \underline{\psi_2^T} \\ \vdots \\ \underline{\psi_n^T} \end{bmatrix} \begin{bmatrix} \underline{\phi_1}, & \underline{\phi_2}, & \cdots, & \underline{\phi_n} \end{bmatrix} = \begin{bmatrix} \underline{\psi_1^T}\underline{\phi_1} & \underline{\psi_1^T}\underline{\phi_2} & \cdots & \underline{\psi_1^T}\underline{\phi_n} \\ \underline{\psi_2^T}\underline{\phi_1} & \underline{\psi_2^T}\underline{\phi_2} & \cdots & \underline{\psi_2^T}\underline{\phi_n} \\ \vdots & \vdots & \ddots & \vdots \\ \underline{\psi_n^T}\underline{\phi_1} & \underline{\psi_n^T}\underline{\phi_2} & \cdots & \underline{\psi_n^T}\underline{\phi_n} \end{bmatrix}. \qquad (56)$$

Consider the case in which k measured modes are available, and l basis vectors are to employed. The calculation of the significant elements of **B** then reduces to

$$\mathbf{B} = \Psi_l^{\mathrm{T}}\Phi_k = \begin{bmatrix} \underline{\psi_1^T} \\ \underline{\psi_2^T} \\ \vdots \\ \underline{\psi_l^T} \end{bmatrix} \begin{bmatrix} \underline{\phi_1}, & \underline{\phi_2}, & \cdots, & \underline{\phi_k} \end{bmatrix} = \begin{bmatrix} \underline{\psi_1^T}\underline{\phi_1} & \underline{\psi_1^T}\underline{\phi_2} & \cdots & \underline{\psi_1^T}\underline{\phi_k} \\ \underline{\psi_2^T}\underline{\phi_1} & \underline{\psi_2^T}\underline{\phi_2} & \cdots & \underline{\psi_2^T}\underline{\phi_k} \\ \vdots & \vdots & \ddots & \vdots \\ \underline{\psi_l^T}\underline{\phi_1} & \underline{\psi_l^T}\underline{\phi_2} & \cdots & \underline{\psi_l^T}\underline{\phi_k} \end{bmatrix}. \qquad (57)$$

Under these conditions the matrix **B** is seen to have k columns and l rows. In keeping with practical ratios of measured modes and basis vectors, l is taken to be larger than k.

If it informative to examine the case in which the unmeasured mode shapes of the matrix Φ are approximated by those of the uniform shear beam, i. e., modes $k+1$ through n are replaced by basis vectors, $\underline{\psi_j}$, with the same index. In this case **B** becomes

$$\mathbf{B} = \left[\begin{array}{cccc:cccc} \underline{\psi_1^T}\underline{\phi_1} & \underline{\psi_1^T}\underline{\phi_2} & \cdots & \underline{\psi_1^T}\underline{\phi_k} & \underline{\psi_1^T}\underline{\psi_{k+1}} & \underline{\psi_1^T}\underline{\psi_{k+2}} & \cdots & \underline{\psi_1^T}\underline{\psi_n} \\ \underline{\psi_2^T}\underline{\phi_1} & \underline{\psi_2^T}\underline{\phi_2} & \cdots & \underline{\psi_2^T}\underline{\phi_k} & \underline{\psi_2^T}\underline{\psi_{k+1}} & \underline{\psi_2^T}\underline{\psi_{k+2}} & \cdots & \underline{\psi_2^T}\underline{\psi_n} \\ \vdots & \vdots & \ddots & \vdots & \vdots & \vdots & \ddots & \vdots \\ \underline{\psi_l^T}\underline{\phi_1} & \underline{\psi_l^T}\underline{\phi_2} & \cdots & \underline{\psi_l^T}\underline{\phi_k} & \underline{\psi_l^T}\underline{\psi_{k+1}} & \underline{\psi_l^T}\underline{\psi_{k+2}} & \cdots & \underline{\psi_l^T}\underline{\psi_n} \\ \hdashline \underline{\psi_{l+1}^T}\underline{\phi_1} & \underline{\psi_{l+1}^T}\underline{\phi_2} & \cdots & \underline{\psi_{l+1}^T}\underline{\phi_k} & \underline{\psi_{l+1}^T}\underline{\psi_{k+1}} & \underline{\psi_{l+1}^T}\underline{\psi_{k+2}} & \cdots & \underline{\psi_{l+1}^T}\underline{\psi_n} \\ \underline{\psi_{l+2}^T}\underline{\phi_1} & \underline{\psi_{l+2}^T}\underline{\phi_2} & \cdots & \underline{\psi_{l+2}^T}\underline{\phi_k} & \underline{\psi_{l+2}^T}\underline{\psi_{k+1}} & \underline{\psi_{l+2}^T}\underline{\psi_{k+2}} & \cdots & \underline{\psi_{l+2}^T}\underline{\psi_n} \\ \vdots & \vdots & \ddots & \vdots & \vdots & \vdots & \ddots & \vdots \\ \underline{\psi_n^T}\underline{\phi_1} & \underline{\psi_n^T}\underline{\phi_2} & \cdots & \underline{\psi_n^T}\underline{\phi_k} & \underline{\psi_n^T}\underline{\psi_{k+1}} & \underline{\psi_n^T}\underline{\psi_{k+2}} & \cdots & \underline{\psi_n^T}\underline{\psi_n} \end{array}\right]. \quad (58)$$

Because Ψ is orthonormal, most of the terms in the upper right and lower right blocks of Eqn. 58 are zero; those of the form $\underline{\psi_m^T}\underline{\psi_m}$ are equal to unity. The upper left block contains the significant elements of **B** as before, whereas the lower left block contains numbers which can be considered discardable noise under the condition that only l basis vectors are meaningful in the expansions of the measured modes. Therefore, Eqn. 58 reduces to

$$\mathbf{B} = \left[\begin{array}{cccc:cccccc} \underline{\psi_1^T}\underline{\phi_1} & \underline{\psi_1^T}\underline{\phi_2} & \cdots & \underline{\psi_1^T}\underline{\phi_k} & 0 & \cdots & \cdots & \cdots & \cdots & 0 \\ \vdots & \vdots & \vdots & & \vdots & \vdots & \vdots & \vdots & \vdots & \vdots \\ \underline{\psi_k^T}\underline{\phi_1} & \underline{\psi_k^T}\underline{\phi_2} & \ddots & \underline{\psi_k^T}\underline{\phi_k} & 0 & \cdots & \cdots & \cdots & \cdots & 0 \\ \underline{\psi_{k+1}^T}\underline{\phi_1} & \underline{\psi_{k+1}^T}\underline{\phi_2} & \cdots & \underline{\psi_{k+1}^T}\underline{\phi_k} & 1 & 0 & \cdots & \cdots & \cdots & 0 \\ \cdots \vdots & \vdots & \ddots & \vdots & 0 & 1 & 0 & \cdots & \vdots & 0 \\ \underline{\psi_l^T}\underline{\phi_1} & \underline{\psi_l^T}\underline{\phi_2} & \cdots & \underline{\psi_l^T}\underline{\phi_k} & \vdots & 0 & \ddots & \ddots & \vdots & \vdots \\ \hdashline 0 & 0 & \cdots & 0 & \vdots & \vdots & \ddots & \ddots & 0 & \vdots \\ \vdots & \vdots & \ddots & \vdots & 0 & 0 & \cdots & 0 & 1 & 0 \\ 0 & 0 & \cdots & 0 & 0 & 0 & \cdots & \cdots & 0 & 1 \end{array}\right]. \quad (59)$$

in which the diagonal string of ones extends from the intersection of the $(k+1)^{st}$ column and row to the lower right corner.

The process of determining **B** from test data is illustrated by the following example using results from experiments on the 12-story Parsons building (Foutch, 1976). The example also helps guide the determination

of general values for l. Three modes were measured in the North-South and East-West directions in the vibration tests of the Parsons building. The matrix **B** for North-South response was first evaluated by using the three normalized measured modes in the North-South direction and the full set of 12 basis vectors. This produces the 12 by 3 matrix given below, with elements rounded to three significant figures. Values of the **B** matrix for $l = 6$ and for $l = 3$ are marked by the dashed lines.

These calculations and those reported for other structures were performed on IIsi, IIci, and 540c Apple computers using the program Excel.

Table 1

NS **B** MATRIX

b_{i1}	b_{i2}	b_{i3}
0.986	–0.212	–0.147
0.168	0.949	–0.077
–0.010	0.226	0.933
0.009	0.031	0.306
0.009	0.019	0.022
0.001	0.022	0.086
–0.006	0.006	0.014
–0.002	0.023	0.019
0.000	0.002	0.019
0.006	0.026	0.005
0.010	–0.013	0.006
–0.002	0.010	–0.008

The twelve-row, six-row and three-row **B** matrices were then used to reconstitute the three normalized measured modes according to Eqn. 11, and the results compared to the normalized measured values. The differences were quantified by taking the square root of the sum of the squares of the differences between the ordinates of the measured modes and the reconstituted modes. This measure, given in Table 2 below, can be compared to unity, since $\underline{\phi_j^T}\,\underline{\phi_j} = 1$.

Table 2

NS MODAL ERRORS

	Mode # 1	Mode # 2	Mode # 3
$l=12$	$5.82\ X\ 10^{-8}$	$5.23\ X\ 10^{-8}$	$5.07\ X\ 10^{-8}$
$l=6$	0.0132	0.0389	0.0326
$l=3$	0.0183	0.0574	0.3202

As expected, using all twelve $\underline{\psi_j}$ vectors produces essentially no error. The error for six $\underline{\psi_j}$ vectors is quite small, and as can be seen for the third mode in Figure 2, the difference between the measured and recomposed mode is not significant, and is within typical measurement error. If the number of $\underline{\psi_j}$ vectors is further reduced to three, giving a square **B** matrix, the differences between the measured and reconstituted modes become unacceptably large, as indicated by the numbers in Table 2, and the plot in Figure 2.

This analysis was repeated for the three measured modes of East-West response with similar results.

As seen in Table 1, the form of the **B** matrix is such that it is relatively easy to calculate it for a larger value of l than is finally used. This approach was used in the data reduction and helped in deciding to use, where not limited by the number of measured levels of response, twice as many basis vectors as measured modes shapes, but not less than six. The **B** matrices calculated from the building test data are included in Appendix II.

After the **B** matrix was formed for each tested direction of response of each building, Eqns. 25, 32, 41 and 51 were used to calculate $p_j, q_j, r_j,$ and s_j' . These calculations were organized by mode, means and standard deviations were calculated, and the results summarized in tabular form. The results are given in Tables 3 through 8, below. The statistics for the sixth modes are not considered reliable and are included for information only. The North-South sixth mode shape determined from ambient tests of the San Diego Gas and Electric building was quite different from the shape used herein, which is from the forced vibration tests (Jennings et. al., 1971). Differences of the type seen in the two tests have been attributed (Trifunac, 1972) to significant contributions of non-resonating modes in the forced vibration tests.

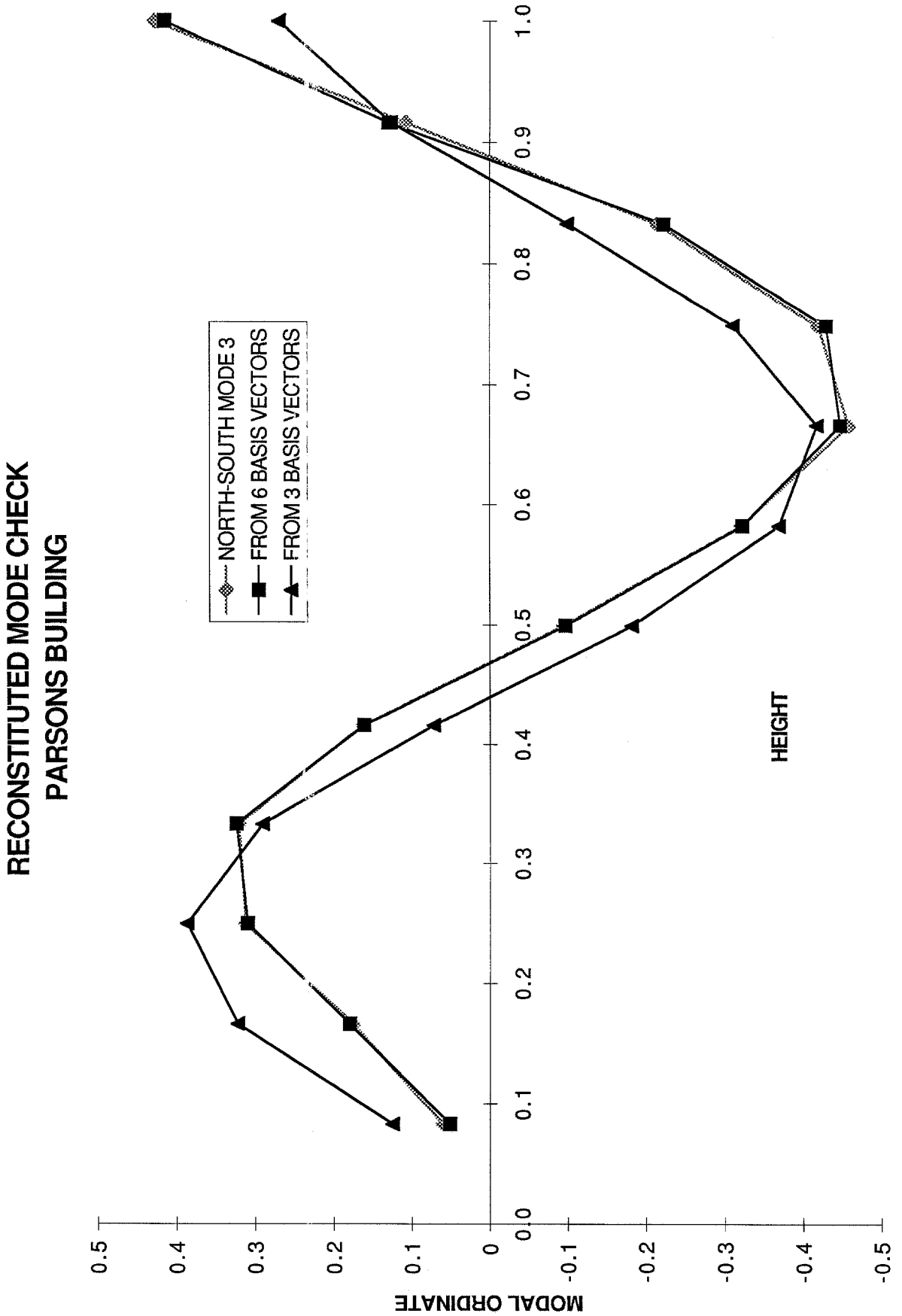

Figure 2. Reconstitution of a measured mode shape from basis vectors

Table 3

SUMMARY OF FIRST MODE DATA

Building	Stories	Direction	p_1	q_1	r_1	s_1'
Imperial Bank-Canada	44	Trans.	0.93	1.25	0.8	1
Century City	42	EW	0.96	0.9	0.84	1
		NS	0.94	0.92	0.81	0.99
Ohbayashi-Gumi-Japan	42	EW	1.01	1.04	1.13	1
Union Bank	38	EW	0.96	1.19	0.91	1.01
		NS	0.98	1.17	0.94	1.01
CIL House-Canada	34	Long.	1	1.14	1.07	1
Alcoa	27	EW	0.92	1.18	0.81	1
		NS	0.99	1.06	0.97	1
San Diego G&E	21	EW	0.97	1.13	0.97	1.01
		NS	0.97	1.02	0.96	1
DIC Building-Japan	18	EW	0.97	1.12	0.92	1.01
		NS	0.96	1.09	0.89	1.01
U. C. Med. Ctr.	15	EW	1	1.09	1.05	1
		NS	0.96	1.27	0.94	1.01
Parsons	12	EW	0.94	1.16	0.82	1.01
		NS	0.93	1.16	0.81	1
JPL Bldg. 180	10	EW	1.03	1	1.11	1
		NS	0.98	1.11	0.97	1.01
Mean			**0.97**	**1.11**	**0.93**	**1.00**
Standard Deviation			**0.029**	**0.096**	**0.101**	**0.006**

Table 4

SUMMARY OF SECOND MODE DATA

Building	Stories	Direction	p_2	q_2	r_2	s'_2
Imperial Bank-Canada	44	Trans.	1.05	1.18	0.69	0.02
Century City	42	EW	1.14	1.12	0.78	0
		NS	1.14	1.14	0.69	0.03
Ohbayashi-Gumi-Japan	42	EW	1.43	0.97	0.87	0.1
Union Bank	38	EW	1.43	1.11	1.02	0.07
		NS	1.3	1.08	1.03	0.01
CIL House-Canada	34	Long.	1.47	0.86	1.2	0.04
Alcoa	27	EW	1.4	0.96	0.87	0.09
		NS	1.46	0.9	1.13	0.05
San Diego G&E	21	EW	1.3	1.01	1.11	0
		NS	1.5	0.79	1.05	0.09
DIC Building-Japan	18	EW	1.34	1.08	0.94	0.05
		NS	1.49	0.93	0.92	0.12
U. C. Med. Ctr.	15	EW	0.2	1.25	0.68	0.36
		NS	0.36	1.18	0.95	0.34
Parsons	12	EW	1.45	1.05	0.9	0.11
		NS	1.46	1.04	0.97	0.1
JPL Bldg. 180	10	EW	1.47	0.98	1.27	0.04
		NS	1.69	0.91	1.24	0.13
Mean			**1.27**	**1.03**	**0.96**	**0.09**
Standard Deviation			**0.37**	**0.12**	**0.17**	**0.10**

Table 5

SUMMARY OF THIRD MODE DATA

Building	Stories	Direction	p_3	q_3	r_3	s'_3
Century City	42	EW	0.86	1.03	0.59	0.01
		NS	0.75	1.03	0.6	0.03
Ohbayashi-Gumi-Japan	42	EW	1.12	0.83	0.89	0
Union Bank	38	EW	0.7	1.08	0.9	0.07
		NS	0.52	1.03	0.75	0.09
CIL House-Canada	34	Long.	0.94	1.08	0.93	0.02
San Diego G&E	21	EW	0.88	0.99	1.11	0.01
		NS	0.63	0.57	0.99	0.12
DIC Building-Japan	18	EW	1.31	1.3	0.98	0.13
		NS	0.77	0.96	0.81	0.07
U. C. Med. Ctr.	15	EW	0.88	1.44	0.55	0.23
		NS	1.12	1.53	0.72	0.24
Parsons	12	EW	0.68	0.98	0.71	0.07
		NS	0.08	1.12	0.49	0.11
JPL Bldg. 180	10	EW	0.5	0.88	1.14	0.13
		NS	0.33	0.66	1.14	0.21
Mean			**0.75**	**1.03**	**0.83**	**0.10**
Standard Deviation			**0.30**	**0.24**	**0.21**	**0.08**

Table 6

SUMMARY OF FOURTH MODE DATA

Building	Stories	Direction	p_4	q_4	r_4	s'_4
Century City	42	EW	1.67	1.1	0.77	0.08
		NS	1.8	1.01	0.77	0.1
Ohbayashi-Gumi-Japan	42	EW	1.26	1.18	0.96	0
Union Bank	38	EW	1.08	0.89	0.95	0.01
		NS	1.2	0.85	1.02	0.01
San Diego G&E	21	EW	2.15	0.43	1.3	0.2
		NS	2.23	0.21	1.1	0.2
U. C. Med. Ctr.	15	EW	1.09	1.64	0.29	0.27
		NS	0.41	1.44	0.63	0.22
JPL Bldg. 180	10	EW	1.01	0.71	1.24	0.05
Mean			**1.39**	**0.95**	**0.90**	**0.11**
Standard Deviation			**0.54**	**0.41**	**0.29**	**0.10**

Table 7

SUMMARY OF FIFTH MODE DATA

Building	Stories	Direction	p_5	q_5	r_5	s'_5
Century City	42	EW	1.7	1.84	0.61	0.13
		NS	1.47	1.68	0.54	0.1
Ohbayashi-Gumi-Japan	42	EW	1.77	1.52	1.04	0.14
Union Bank	38	EW	1.02	0.88	1.01	0.03
		NS	0.69	0.88	0.88	0.04
San Diego G&E	21	EW	0.19	0.9	0.94	0.08
		NS	0.88	0.46	0.7	0.21
U. C. Med. Ctr.	15	EW	1.23	1.88	0.32	0.23
		NS	1.04	1.91	0.41	0.21
Mean			**1.11**	**1.33**	**0.72**	**0.13**
Standard Deviation			**0.47**	**0.52**	**0.25**	**0.07**

Table 8

SUMMARY OF SIXTH MODE DATA

Building	Stories	Direction	p_6	q_6	r_6	s'_6
Century City	42	EW	1.4	1.94	0.49	0.28
San Diego G&E	21	EW	0.65	1.36	0.38	0.01
		NS	3.31	2.47	0.14	0.47
Mean			**1.79**	**1.92**	**0.34**	**0.25**
Standard Deviation			**1.12**	**0.45**	**0.15**	**0.19**

From Eqn. 24 one sees that the role of the parameter p_j is to modify the participation factor, α_j, as the modes of the structure under consideration differ from those of a uniform shear beam. Table 3 shows that the first modes of the tall buildings have an average value of p_1 just under unity, with a standard deviation of only 3 per cent. Table 4 shows that the average value of p_2 is 1.27, and Table 5 lists an average value of p_3 of 0.75. These figures indicate that the second modes of tall buildings, on average, consistently respond more to earthquake excitation than the second mode of a uniform shear beam, and the third modes consistently less than the corresponding mode of the shear beam. Similar implications can be drawn for the higher modes, although with less confidence because of the sparseness of the data. Predictably, the standard deviation of p_j is much larger for the higher modes than it is for the first mode, reflecting differences among the buildings and, for the higher modes, inaccuracies in the data and the small size of the sample.

The parameter q_j arises in the determination of the displacement and acceleration at the roof of the structure. As shown by Eqns. 31 and 55, the influence of the mode shapes is reflected in the product $p_j q_j$. Tables 3 through 8 show that the average q_j is within 10 percent of unity for the first four modes, with the standard deviation growing with increasing mode number. The sparse data for the fifth mode, and possibly for the

sixth mode, suggest that the average q_j may be larger for these higher modes.

Equation 35 shows that the modal base shear differs from that for a uniform shear beam as the factor p_j^2 differs from unity. When squared, the differences from unity of the average values of p_j discussed above for the second and third modes become accentuated. The values of p_j^2 indicate that on average the second mode contribution to base shear is about 1.6 times that of a uniform shear beam, while the third mode is only a little more than half its counterpart.

The factor r_j modulates the modal drift at the base of the structure through the product $p_j r_j$ in Eqn. 40. The effect is a small reduction as the average values for r_j in Tables 3 through 8 are all less than unity, with a consistent tendency to decrease with increasing mode number. The standard deviation of r_j is only 0.10 for the first mode, but increases to 0.20 or more for higher modes.

The modal contribution to base moment is given by Eqn. 52 which contains the product $p_j s_j'$. The results in Tables 3 show $s_1' = s_1$ to be essentially unity with a standard deviation of less than one per cent, while figures in Tables 4 through 8 indicate that the average value of s_j' is near 0.10 for the higher modes.

The parameters p_j, q_j, r_j and s_j' weigh in different manners the contributions of the basis vectors to the modal quantity in question. These contributions reflect, in turn, the geometry of the mode shape, specifically, how it differs from the corresponding mode shape of the uniform shear beam as measured by the appropriate column of the **B** matrix. Examination of the tables shows some interesting cases. For example, in Table 3 q_1 for the University of California Medical Center is near the mean for the East-West direction, but the value for the North-South direction is the highest in the sample. Comparing the values of the corresponding columns of the **B** matrices in Appendix II shows that the North-South first mode has much higher values for the contributions of the second and third basis vectors than does the East-West mode. The plots given in the report of the vibration test (Rea et. al., 1966) show that this is a consequence of modal geometry: the North-South fundamental mode is rather wavy, while the East-West fundamental mode is nearly a straight line. Another example is given by p_2 for the Jet Propulsion Laboratory

Building 180 in Table 4. The value for the North-South direction is the highest given, while the value for the East-West direction is only slightly higher than average. Comparing the corresponding **B** matrices shows much more contribution to the second mode shape from the first and third basis vectors in the North-South direction than in the East-West direction, differences that can be seen in the mode shapes. The test data (Nielsen, 1964) show the two maxima of the East-West mode to be about the same, as they are for a shear beam, whereas the lower maximum is significantly larger than the upper one for the North-South direction.

Not all of the reasons for differences are so clear; the very low values for p_2 shown by the University of California Medical Center in Table 4 are not reflective of such obvious differences in the **B** matrices or in the plots of the mode shapes (Rea et. al., 1966).

The next chapter illustrates the application of the four basic parameters p_j, q_j, r_j and s_j' to the earthquake response of tall buildings.

CHAPTER V--EARTHQUAKE RESPONSE

Introduction

The analysis of the first chapter can now be combined with the reduced data from the second chapter to produce quantitative expressions for averages of important measures of earthquake response. The reason this is feasible is that tall buildings share closely many of the properties that determine their response to earthquake motion, as shown by the results of the previous chapter. The variation among these properties measured by the parameters p_j, q_j, r_j and s_j' , while significant, is quite small for the fundamental mode; it becomes correspondingly larger for the higher modes, but the importance of the higher modes to earthquake response correspondingly decreases. Also, it is important to note that the variations among the structural parameters governing the earthquake response appear to be much smaller than the variation in the expected response spectrum ordinates, even given a fixed magnitude and distance for the earthquake under consideration.

There is another shared property of tall buildings that can be used to advantage in estimating their earthquake response. Table 9 gives the measured periods of the tall buildings included in this study (Burridge and Nalbandian, 1983; Jennings, 1969). The values show that the period ratios of tall buildings have well-defined average values which increase almost like the odd integers that characterize the uniform shear beam.

Table 9

RATIOS OF HIGHER PERIODS TO FUNDAMENTAL PERIOD

RATIOS OF MEASURED BUILDING PERIODS

Building	Stories	Direction	T_1/T_2	T_1/T_3	T_1/T_4	T_1/T_5	T_1/T_6
Imperial Bank-Canada	44	Trans.	2.91	5.07	7.72	9.63	11.91
		Long.	2.73	4.79	7.07	8.93	11.07
Century City	42	EW	2.85	4.93	7.08	10.26	11.72
		NS	2.93	5.14	7.39	10.67	11.80
Ohbayashi-Gumi-Japan	42	EW	3.03	5.13	9.09	11.11	
Union Bank	38	EW	3.03	5.58	7.95	10.49	
		NS	2.90	5.09	7.17	9.25	
CIL House-Canada	34	Long.	2.84	5.04	7.36	9.84	
		Trans.	3.05	5.58	8.26	11.16	13.48
Alcoa	27	EW	3.10				
		NS	2.82				
San Diego G&E	21	EW	3.05	5.76	8.63	11.32	13.45
		NS	2.88	5.21	7.85	10.73	13.35
DIC Building-Japan	18	EW	2.92	5.03			
		NS	2.94	5.54			
U. C. Med. Ctr.	15	EW	2.65	4.59	6.53	8.47	
		NS	2.65	4.59	6.53	8.47	
Parsons	12	EW	2.77	4.54			
		NS	2.60	4.07			
JPL Bldg. 180	10	EW	2.97	5.02	7.43		
		NS	3.30	6.44			
Average Value			**2.90**	**5.11**	**7.58**	**10.03**	**12.40**
Value for a Uniform Shear Beam			**3**	**5**	**7**	**9**	**11**
Ratio			**0.97**	**1.02**	**1.08**	**1.11**	**1.13**

Because the parameters p_j, q_j, r_j and s_j' occur in various products in determining maximum displacement, base shear, etc., it is convenient to introduce the means and standard deviations given in Table 10. The format in this table is mean ± standard deviation.

Table 10

MEANS AND STANDARD DEVIATIONS OF PRODUCTS

MEANS AND STANDARD DEVIATIONS
$p_j q_j$, p_j^2, $p_j r_j$, and $p_j s_j'$

	$p_j q_j$	p_j^2	$p_j r_j$	$p_j s_j'$
First Mode	1.07 ±0.09	0.94 ±0.06	0.91 ±0.12	0.97 ±0.03
Second Mode	1.27 ±0.34	1.74 ±0.69	1.26 ±0.48	0.09 ±0.06
Third Mode	0.81 ±0.45	0.66 ±0.44	0.63 ±0.29	0.07 ±0.07
Fourth Mode	1.16 ± 0.5	2.22 ±1.53	1.32 ±0.76	0.16 ±0.16
Fifth Mode	1.63 ±1.05	1.46 ±1.01	0.77 ±0.46	0.15 ± 0.1

The response of higher modes to the total earthquake response is addressed in the following calculations by using the averaged measured properties of tall buildings for the first five modes and approximating the properties of the next five modes by those of the uniform shear beam. The variations are approximated by using the standard deviations of Table 10 for the first five modes, while for the higher modes a standard deviation equal to the mean was employed. The modal contributions are combined to give the total value by the familiar approach of taking the square root of the sum of the squares (SRSS) of the individual modal contributions (Rosenblueth, 1951; Chopra, 1995). Other assumptions and features of the approach are introduced in the presentation of the results, which follow the order of the second chapter.

Displacement at the Roof of the Structure

The modal contributions to the displacement of the roof of the structure are given by Eqn. 31, repeated here for convenience with an equal sign,

$$u_{nj}(\max) = \frac{2T_j}{\pi^2(2j-1)} S_{pv}(T_j, \zeta_j) p_j q_j. \tag{60}$$

Introducing the ratio of periods

$$T_j = \frac{T_1}{(2j-1)} \tag{61}$$

and rearranging,

$$u_{nj}(\max) = \frac{2T_1}{\pi^2} S_{pv}(T_j, \zeta_j) \frac{p_j q_j}{(2j-1)^2}. \tag{62}$$

The total displacement is found by combining the contributions of the modes by some combination rule, R_k, wherein k denotes the number of modes employed in the combination. As mentioned above, modal contributions are combined in this study by the SRSS rule.

Design spectra for major and great earthquakes are usually nearly constant for periods from one to several seconds, reflecting measured properties of strong ground motion. This implies that S_{pv} is about the same for the first few modes of a tall building; it then decreases for higher modes. This feature, and the fact that the modal contributions to the maximum displacement decrease rapidly with mode number permits the introduction of the approximation

$$S_{pv}(T_j, \zeta_j) \approx S_{pv}(T_1, \zeta_1). \tag{63}$$

Equation 63 overestimates the contributions of the higher modes, but as will be seen, this usually has little affect on the combined result. It also assumes the damping is the same in all the modes. Of course, the assumptions involved in Eqns. 61 and 63 do not have to be made if building periods and dampings are known and a specific spectrum has been determined.

Combining the above,

$$u_n(\max) = \frac{2T_1}{\pi^2} S_{pv}(T_1, \zeta_1) R_k\left(\frac{p_j q_j}{(2j-1)^2}\right) \tag{64}$$

The following table shows the modal contributions and their combined value using the average values of $p_j q_j$ from Table 10 for the

first five modes. The combination is repeated for ten modes, using shear beam properties for modes six through ten.

Table 11

MODAL CONTRIBUTIONS TO MAXIMUM ROOF DISPLACEMENT

MAXIMUM ROOF DISPLACEMENT

mode	$p_j q_j$ mean	$p_j q_j$ sigma	$\frac{\text{mean}}{(2j-1)^2}$	$\frac{\text{sigma}}{(2j-1)^2}$
1	1.07	0.09	1.0700	±0.0900
2	1.27	0.34	0.1411	±0.0378
3	0.81	0.45	0.0324	±0.0180
4	1.16	0.5	0.0237	±0.0102
5	1.63	1.05	0.0201	±0.0130
6	1	1	0.0083	±0.0083
7	1	1	0.0059	±0.0059
8	1	1	0.0044	±0.0044
9	1	1	0.0035	±0.0035
10	1	1	0.0028	±0.0028
		R_5	1.08	± 0.10
		R_{10}	1.08	± 0.10

The factor ± 0.10 associated with R_5 in Table 11 and a similar factor associated with R_{10} are calculated by taking the square root of the sum of the squares of the standard deviations of $p_j q_j$ given in the last column of the table. These ± factors are not true standard deviations, but do give an indication of the variation that can be expected as a result of variations in the individual modal contributions.

The results in Table 11 show that to three significant figures, the calculated maximum displacement is the same whether five modes are used, or ten. The use of shear beam properties to represent the contributions of modes 6-10 may underestimate or overestimate the contributions of individual higher modes, but such inaccuracies do not affect the final result.

Combining the values for R_{10} from Table 11 with Eqn. 64 gives the following,

$$u_n(\max) = 0.22\, T_1\, S_{pv}(T_1, \zeta_1). \tag{65}$$

Equation 65 applies directly to small earthquake excitation, but for larger motions T_1 should be interpreted as the period appropriate to strong earthquake response.

If the variation given in Table 11 is carried through to Eqn. 65, a value of ± 0.093 results. However, to include this in the equation would be potentially misleading as this figure of approximately 10 per cent does not include variations resulting from Eqn. 61 or other assumptions, sources which undoubtedly increase the variation in Eqn. 65 attributable to structural sources. Even so, it is thought that the total of structurally-caused variations still does not approach the much larger variations in Eqn. 65 inherent in the response or design spectrum, $S_{pv}(T_1, \zeta_1)$. Studies show that the response spectrum from a major earthquake can easily vary a factor of two or more about the mean, even for a given earthquake magnitude and distance (Takeo and Kanamori, 1992; Kanamori, 1996).

Base Shear

The maximum base shear is one of the most important results of earthquake response studies, giving as it does the largest total force resisted by the building. In addition, the design base shear is a fundamental parameter in building codes and in most approaches to earthquake resistant design. The maximum base shear in the j^{th} mode of response, as a fraction of the weight of the structure, is given by Eqn. 35, taken as an equality,

$$\frac{V_j}{m_0 g}(\max) = \frac{16}{\pi g (2j-1)^2 T_j} S_{pv}(T_j, \zeta_j) p_j^2. \tag{66}$$

Introducing Eqn. 61 and rearranging gives

$$\frac{V_j}{m_0 g}(\max) = \frac{16}{\pi g T_1} S_{pv}(T_j, \zeta_j) \frac{p_j^2}{(2j-1)}. \tag{67}$$

Again, note that for tall buildings S_{pv} will be about the same for the first few modes, then decreasing for the higher modes. Introducing Eqn.

63 conservatively approximates the small contribution to base shear of these higher modes. Combining the maximum for each mode yields the maximum base shear,

$$\frac{V}{m_0 g}(\max) = \frac{16}{\pi g T_1} S_{pv}(T_1, \zeta_1) R_k \left(\frac{p_j^2}{(2j-1)} \right). \tag{68}$$

Table 12 gives the modal contributions to maximum base shear and the combination for five modes and for ten. The values for p_j^2 are taken from table 10 for the first five modes and shear beam properties are used for modes six through ten.

Table 12

MODAL CONTRIBUTIONS TO MAXIMUM BASE SHEAR

mode	p_j^2 mean	p_j^2 sigma	MAXIMUM BASE SHEAR mean $/(2j-1)$	sigma $/(2j-1)$
1	0.94	0.06	0.9400	±0.0600
2	1.74	0.69	0.5800	±0.2300
3	0.66	0.44	0.1320	±0.0880
4	2.22	1.53	0.3171	±0.2186
5	1.46	1.01	0.1622	±0.1122
6	1	1	0.0909	±0.0909
7	1	1	0.0769	±0.0769
8	1	1	0.0667	±0.0667
9	1	1	0.0588	±0.0588
10	1	1	0.0526	±0.0526
		R_5	1.17	± 0.35
		R_{10}	1.18	± 0.39

The format of Table 12 is the same as Table 11 and the ± values associated with R_5 and R_{10} have the same meaning. Although the fundamental mode is the predominant contributor to base shear, it does not dominate as it does for the roof deflection. This reflects the different powers of the factor $(2j-1)$ in Eqns. 64 and 68. For the maximum base shear the first few modes all make significant contributions and the

variation of the combined result is larger than would be the case if a single mode dominated. The results in Table 12 also show that modes six through ten make measurable, but insignificant, contributions to the combined total, indicating that approximating their contributions by those of shear beam modes is acceptable.

Using the result for R_{10} in Eqn. 68 yields

$$\frac{V}{m_0 g}(\max) = 6.0\,\frac{S_{pv}(T_1,\zeta_1)}{gT_1}. \tag{69}$$

Equation 69 is in a convenient form for applications; only the response or design spectrum and the fundamental period are required to produce a numerical estimate for the maximum base shear.

First Story Drift

The development of a similar expression for the first story drift begins with Eqn. 40, with equality assumed

$$d_{1j}(\max) = \frac{T_j}{\pi l} S_{pv}(T_j,\zeta_j) p_j r_j. \tag{70}$$

Applying Eqns. 61 and 63 an proceeding as above gives

$$d_{1j}(\max) = \frac{T_1}{\pi l} S_{pv}(T_1,\zeta_1) \frac{p_j r_j}{(2j-1)}, \tag{71}$$

and combining the modes yields

$$d_1(\max) = \frac{T_1}{\pi l} S_{pv}(T_1,\zeta_1) R_k\left(\frac{p_j r_j}{(2j-1)}\right). \tag{72}$$

The modal contributions and their combination are given below in Table 13. Again the properties of the first five modes are taken from the building data, while shear beam properties are used for modes six through ten.

Table 13

MODAL CONTRIBUTIONS TO FIRST STORY DRIFT

MAXIMUM FIRST STORY DRIFT

mode	$p_j r_j$ mean	$p_j r_j$ sigma	mean $(2j-1)$	sigma $(2j-1)$
1	0.91	0.12	0.9100	±0.1200
2	1.26	0.48	0.4200	±0.1600
3	0.63	0.29	0.1260	±0.0580
4	1.32	0.76	0.1886	±0.1086
5	0.77	0.46	0.0856	±0.0511
6	1	1	0.0909	±0.0909
7	1	1	0.0769	±0.0769
8	1	1	0.0667	±0.0667
9	1	1	0.0588	±0.0588
10	1	1	0.0526	±0.0526
		R_5	1.03	± 0.24
		R_{10}	1.04	± 0.29

The same pattern of modal contributions is seen for the first story drift as was seen for the base shear. The first few modes all contribute significantly, although the largest contribution comes from the first mode. Very little is contributed by modes six through ten.

Combining the values for R_{10} with Eqn. 72 produces the equation

$$d_1(\max) = 0.33 \frac{T_1 S_{pv}(T_1, \zeta_1)}{l}. \tag{73}$$

The SRSS combination is based on a statistical approach in which the modes are taken to respond independently. If the earthquake motion is a short pulse-like motion, then the modes do not respond independently, several of them are locked in phase with each other to produce a deflection wave that progresses up the structure. Simulations (Hall et. al., 1996) show this large deflection wave is especially important for interstory drift. In the present context, this situation can be approximated by taking the sum of

the involved modal contributions; in effect this assumes that the modes add up in phase at the first story to start the wave that progresses up the structure. If the first five modes are added, R_5 becomes 1.73, rather than 1.03. If this approach is considered valid, the coefficient in Eqn. 73 would increase accordingly.

Base Moment

The calculation of Base moment begins with Eqn. 52,

$$\frac{H_j}{m_0 g l}(\max) = \frac{32}{\pi^2 g (2j-1) T_j} S_{pv}(T_j, \zeta_j)\, p_j s'_j. \tag{74}$$

Because s'_j incorporates a factor of $(2j-1)^{-2}$, the contributions of the higher modes decreases very rapidly with mode number. Even after using Eqns. 61 and 63, i.e.,

$$\frac{H_j}{m_0 g l}(\max) = \frac{32}{\pi^2 g T_1} S_{pv}(T_1, \zeta_1)\, R_k(p_j s'_j), \tag{75}$$

the modal contributions decrease as rapidly as they do for the roof displacement. Table 14 shows the modal contributions and their combination in the same way as in previous tables. Using the result for R_{10},

$$\frac{H}{m_0 g l}(\max) = 3.2 \frac{S_{pv}(T_1, \zeta_1)}{g T_1}. \tag{76}$$

Table 14

MODAL CONTRIBUTIONS TO MAXIMUM BASE MOMENT

MAXIMUM BASE MOMENT

mode	$p_j s'_j$ mean	$p_j s'_j$ sigma
1	0.97	± 0.03
2	0.09	± 0.06
3	0.07	± 0.07
4	0.16	± 0.16
5	0.15	± 0.10
6	0.0083	±0.0083
7	0.0059	±0.0059
8	0.0044	±0.0044
9	0.0035	±0.0035
10	0.0028	±0.0028
R_5	1.00	± 0.21
R_{10}	1.00	± 0.21

The shear beam properties of modes six through ten are seen in Table 14 to be much smaller than the pattern that might be inferred from the first few modes. However, if the contributions of modes six through ten are increased ten-fold, R_{10} only increases to 1.01 and the approximation to its variation changes only from 0.21 to 0.24.

The fundamental modes of many tall buildings lack significant curvature and are nearly straight lines. Bielak (1969) has shown that the orthogonality of the modes requires the contribution of the higher modes to base moment to be zero when the fundamental mode is a straight line. The pattern seen in Table 14 reflects this result in general terms, although the average contributions of the fourth and fifth modes are larger than one might expect.

Roof Acceleration

Taking equality in Eqn. 55 and using Eqn. 61,

$$a_{nj}(\max) = \frac{8}{T_1} S_{pv}(T_j, \zeta_j)\, p_j\, q_j. \tag{77}$$

For the acceleration at the roof of the building, the contributions of the higher modes do not intrinsically decrease rapidly. The factor $p_j q_j$ is approximately unity and there is no factor of $(2j-1)$ in the denominator. In this case, it is inappropriate to assume that the spectral ordinates are equal and Eqn. 63 cannot be used. Instead, it is assumed that the first l spectral ordinates are the same, i.e., Eqn. 63 holds for $j = 1, \cdots, l$. The spectral ordinates for the higher modes are assumed to follow a constant acceleration spectrum, that is to be proportional to the period. The break point is taken at $T = 0.5$. These approximations were suggested by approaches used in building codes. Under these conditions,

$$\begin{aligned} S_{pv}(T_j, \zeta_j) &= S_{pv}(T_1, \zeta_1) \qquad j = 1, \ldots, l \\ S_{pv}(T_j, \zeta_j) &= 2T_j\, S_{pv}(T_1, \zeta_1) \quad j = l+1, \ldots, n. \end{aligned} \tag{78}$$

Using Eqn. 78, the modal contributions can be combined by the following relation,

$$a_n(\max) = 16\, S_{pv}(T_1, \zeta_1)\, R_k\left(\frac{p_1 q_1}{2T_1}, \cdots, \frac{p_l q_l}{2T_1}, \frac{p_{l+1} q_{l+1}}{2l+1}, \cdots, \frac{p_k q_k}{(2k-1)}\right). \tag{79}$$

To illustrate how the modes contribute and combine, Table 15 was prepared for the case of $T_1 = 4$ seconds, which implies $l = 4$.

Table 15

MODAL CONTRIBUTIONS TO MAXIMUM ROOF ACCELERATION

MAXIMUM ROOF ACCELERATION

mode	$p_j q_j$ mean	$p_j q_j$ sigma	$2T_1$ or $(2j-1)$	mean / $(2j-1)$	sigma / $(2j-1)$
1	1.07	0.09	8	0.1338	±0.0113
2	1.27	0.34	8	0.1588	±0.0425
3	0.81	0.45	8	0.1013	±0.0563
4	1.16	0.5	8	0.1450	±0.0625
5	1.63	1.05	9	0.1811	±0.1167
6	1	1	11	0.0909	±0.0909
7	1	1	13	0.0769	±0.0769
8	1	1	15	0.0667	±0.0667
9	1	1	17	0.0588	±0.0588
10	1	1	19	0.0526	±0.0526
			R_5	0.33	± 0.15
			R_{10}	0.36	± 0.22

The figures in Table 15 show that including modes six through ten results in about a ten per cent increase in the combined roof acceleration, and about a fifty per cent increase in the variation. Clearly, the higher modes are more important to the roof acceleration than they are to any of the other modal quantities that have been presented. The strong presence of higher mode is confirmed by records of earthquake response obtained from the roofs of tall buildings (Darragh et. al., 1994; Shakal et. al., 1994; Shakal and Huang, 1994; Foutch et. al., 1995).

An Example

To illustrate the application of these results, consider the case of a representative tall building subjected to earthquake motions of the level experienced in the Northern San Fernando Valley in the 1995 Northridge earthquake. The fundamental period of the building at earthquake response levels is estimated to be five seconds. The effective damping factor is taken to be 10 percent of critical, a level associated with non-structural damage

and minor structural damage (McVerry, 1979), but not serious failure or collapse. Examination of response spectra from the Northridge earthquake (Darragh et. al., 1994; Porcella et. al., 1994; Shakal et. al., 1994; Shakal and Huang, 1994) suggests a value of $S_{pv}(T_1, \zeta_1)$ of 50 inches/ second as representative of the motion in the Northern San Fernando Valley for the chosen level of damping. This level, though indicative of quite strong shaking, is only about one-half of the level calculated for a magnitude $M_W = 7.0$ earthquake at site C5 in this region by Hall et. al. (1996).

The only other parameter needed is the height of the building, used in the calculation of first story drift. The value selected is 500 feet.

With the spectral level fixed, and the height and fundamental period selected, Eqns. 65, 69, 73, and 76 can be applied to determine the maximum roof displacement, base shear, first story drift and base moment. The calculation of maximum roof acceleration employs Eqns. 78 and 79, with $l = 5$, and proceeds along the lines of Table 15. The results are summarized below:

Maximum roof displacement	4.6 ft.
Maximum base shear	$0.156 m_0 g$
Maximum first story drift	1.4 per cent
Maximum base moment	$0.084 m_0 g l$
Maximum roof acceleration	$0.65 g$

Although these levels of response are high, they are directly supported by records from strong earthquakes. Base shears, from the fundamental mode only, of the order of 15 per cent of the weight of the structure, were calculated from measured responses obtained in the San Fernando earthquake (Housner and Jennings, 1982, Figure 15), and maximum roof accelerations in the range of $0.65 g$ were recorded in several tall buildings during the Northridge earthquake (Shakal and Huang, 1994; Hall, 1995).

The levels of calculated response are reduced by choosing a higher level of effective damping, but taking 15 per cent rather than 10 per cent, for example, results in only about 20 per cent reduction and begins to call into question whether the structural damage associated with this higher level of equivalent damping can be termed successful response. An increase in the estimated fundamental period reduces the expected maximum base shear, base moment, and roof acceleration, but increases the maximum roof displacement and first story drift.

CHAPTER VI--DISCUSSION AND CONCLUSIONS

The application of the results of this study to strong earthquake motions requires that the building response be linear or, more generally, describable as linear, with equivalent values of periods and dampings. In considering this requirement, one should first reflect on how really important tall buildings are, not only because they house thousands of workers during office hours, but because of what they represent. Tall buildings are the symbols of a modern city and, as such, are a crowning achievement of structural engineering. It is certainly important that tall buildings respond successfully to strong earthquake shaking. In the author's judgment, successful response implies that structural damage is not severe and concentrated, but is distributed over the structure and is sufficiently moderate that the building can reasonably be repaired and brought back into service. Although this level of response is fundamentally non-linear, it is describable as linear, with effective values of periods and dampings. As a case in point, system identification methods using equivalent linear models have been successfully applied to records from damaged structures (Beck, 1982; McVerry, 1979), showing that period elongation of the order of one hundred per cent and equivalent damping values of around 15 to 20 percent are associated with degrees of damage that are, arguably, not acceptable for structures as important as tall buildings. Such considerations support the position that the results of this study can be applied to the desired, successful levels of earthquake response of tall buildings to strong ground motion. The approach is not applicable if failure, highly localized serious damage, or similar measures of severe non-linear response occur or are expected, but such features are not likely to be associated with intended earthquake response.

The study attempts to quantify the variations in results that arise from variations among the mode shapes and frequency ratios of tall buildings, but does not address the variations introduced as a consequence of the assumption of uniformity of floor mass, from uncertainties in determining the equivalent period and damping, etc. It is difficult to quantify these additional, structurally-based variations, but it is believed that the total variation in the final results from structural origins is considerably less than the total of variations attributable to geophysical causes. These include uncertainties in the location, magnitude and source parameters of future earthquakes, as well as the large variations in response spectrum ordinates for a given magnitude and distance.

The results include the determination of the contribution of the higher modes to the response of tall buildings, in an average sense. The results for all the measures of earthquake response investigated, except for the acceleration on the roof, showed that the responses of higher modes, herein modes greater than five, were not significant to the overall response. This conclusion is partially dependent on the method by which the modal contributions are combined, but examination of the modal figures in Tables 11 through 15 shows that whatever the combination method, modes beyond the fifth are unlikely to be important beyond the ten per cent level, except again for the roof acceleration, if the levels of S_{pv} are comparable for all the modes. As a consequence of the wide variation with period of response spectrum ordinates of individual earthquakes, as opposed to the limited variation shown by averaged or smoothed spectra, studies of measured earthquake response sometimes show, for example, a larger contribution to base shear by a higher mode than by the fundamental (Housner and Jennings, 1982). Such variations from the norm clearly can occur but are not characteristic of the most probable response.

Although the use of shear beam mode shapes as basis vectors is a rather obvious choice for tall, regular buildings, other basis vectors may prove advantageous for other classes of structures. For example, the odd-numbered Legendre polynomials have been suggested as models for the mode shapes of some tall buildings (Bielak, 1969). They represent another possible choice for the columns of Ψ. Legendre's equation suggests that these might be useful, for example, in studies of tapered buildings. Another possible extension of the study in this direction would be to replace the average values of p_j, q_j, r_j, and s_j' with values determined from representative, or "generic" mode shapes. Starting with a fundamental mode which is a straight line, a second and third mode have been constructed using orthogonality and the observed location of nodes of structural modes. The process could be continued to generate a larger set of generic modes, but the value of such a set would be much increased if an additional parameter describing the curvature of the fundamental mode could be introduced.

The Northridge and Kobe earthquakes have shown convincingly the destructive power of large, long-period pulses in the ground motions, pulses that recent records have shown are often present in the near field motions of major earthquakes. An important parameter for the response of tall buildings to these pulses is the approximate period of the ground pulse in comparison to the natural periods of the structure. Recognizing that the worst modal excitation for a given energy content is the impulse

response function administered in reverse (Drenick, 1970), and that the fundamental mode is the largest contributor to deflection, drift, base shear, etc., the most demanding case for a tall building would be for the ground motion pulse to be composed of emergent acceleration waves with the same period as the effective period of the fundamental mode. This situation can be modeled in the present context by considering a realistically shaped pulse with a predominant period equal to the equivalent fundamental period of the building and by calculating its response spectrum for the equivalent damping of the structure. A conservative first estimate of the response to the ground motion pulse is achieved by combining the absolute values of the modal responses for the first few modes, i. e., considering them locked in phase constructively. Using five modes in the case of the simple example given above raises the base shear about 80 per cent above the value of $0.156 m_0 g l$ calculated by combining modes by the square root of the sum of the squares. This is for the same level of the response spectrum. Although oversimplified, this quick calculation does give further credence to the importance of understanding the response of tall buildings to impulsive ground motion.

The results given above appear to be amenable to construction of the kinds of graphs and tables needed for systematic approaches to hazard analysis and the determination of seismic design criteria. For example, the results could be combined with suitable damage criteria and the statistical properties of response spectra of scenario earthquakes to aid the estimation of risk to a major city from the response of its tall buildings. Similarly, the results could be combined with formulas for period vs. height and with spectra representing several damping levels of design earthquakes to form convenient tools for estimating earthquake demand for preliminary design of tall buildings.

The approach used in this study could also be applied in the formulation of code provisions for tall buildings, for example, in the context of a performance-based design code. Rather than reducing the design earthquake forces to unrealistically low levels in anticipation of ductile behavior, the response of the building to earthquake forces of different levels of probable occurrence could be calculated using levels of equivalent damping that are representative of the desired level of performance. Appropriate values of equivalent damping could range, for instance, from about 2 per cent for no damage up to about 20 percent for structural damage approaching failure. Such an approach could be rationally improved and updated as measurements of earthquake response of tall buildings accumulate.

ACKNOWLEDGMENTS

The author wishes to acknowledge the support of the California Institute of Technology for the sabbatical leave that made it possible to undertake this study. The National Science foundation provided support for the data collection efforts of Paul Burridge and Armineh Nalbandian, under grant CEE 8119962.

REFERENCES

Beck, J. L. (1978). "Determining Models of Structures from Earthquake Records" Earthquake Engineering Research Laboratory Report 78-01, California Institute of Technology, Pasadena, California.

Bielak, J. (1969). "Base Moment for a Class of Linear Systems" *Journal of the Engineering Mechanics Division*, American Society of Civil Engineers, Vol. 95, No. 5, Oct. 1969, pp. 1053-1062.

Biot, M. A. (1932). *Transient Oscillations in Elastic Systems*, Doctoral thesis, California Institute of Technology, Pasadena, California.

Burridge, Paul and Armineh Nalbandian (1983). "MDSHP-Mode Shapes and Natural Frequencies", unpublished notes, California Institute of Technology, Pasadena, California.

Chopra, A. K. (1995). *Dynamics of Structures*, Prentice-Hall, Englewood Cliffs, New Jersey.

Chopra, A. K. (1996). "Modal Analysis of Linear Dynamic Systems: Physical Interpretation", *Journal of Structural Engineering*, American Society of Civil Engineers, Vol. 122, No. 5, May 1996, pp. 517-527.

Darragh, R., T. Cao, V. Graizer, A. Shakal and M. Huang (1994). "Los Angeles Code-Instrumented Building Records from the Northridge, California Earthquake of January 17, 1994: Processed Release No. 1", California Strong Motion Instrumentation Program, California Department of Conservation, Division of Mines and Geology Office of Strong Motion Studies, Sacramento, California.

Drenick, R. F. (1970). "Model-Free Design of Aseismic Structures", *Journal of the Engineering Mechanics Division*, American Society of Civil Engineers, Vol. 96, No. 4, Aug. 1970, pp. 483-493.

Foutch, D. A., G. W, Housner and P. C. Jennings (1975). "Dynamic Responses of Six Multistory Buildings During the San Fernando Earthquake", Earthquake Engineering Research Laboratory Report 75-02, California Institute of Technology, Pasadena, California.

Foutch, D. A. (1976). "A Study of the Vibrational Characteristics of Two Multistory Buildings", Earthquake Engineering Research Laboratory, Report 76-03, California Institute of Technology, Pasadena, California.

Hall, J. F., T. H. Heaton, M. W. Halling and D. J. Wald (1996). "Near-Source Ground Motion and its Effects on Flexible Buildings", *Earthquake Spectra*, Vol. 11, No. 4, pp. 569-605.

Hall, J. F., Ed. (1995). "Northridge Earthquake Reconnaissance Report, Vol. 1, Chapter 2, Recorded Ground and Structure Motions", *Earthquake Spectra*, Supplement C to Vol. 11, pp. 13-96.

Housner, G. W. (1970). "Strong Ground Motion", in *Earthquake Engineering*, R. L. Weigel, Ed., Prentice-Hall, Englewood Cliffs, New Jersey.

Housner, G. W., and P. C. Jennings (1982). *Earthquake Design Criteria*, Earthquake Engineering Research Institute, Berkeley, California.

Iwan, W. D. (1994). "Near-Field Considerations in Specification of Seismic Design Motions for Structures", *Proceedings of the 10th European Conference on Earthquake Engineering*, Vienna, Austria.

Iwan, W.D. (1996). "The Drift Demand Spectrum and its Application to Structural Design and Analysis", Paper No. 1116, *Proceedings of the Eleventh World Conference on Earthquake Engineering*, Acapulco, Mexico.

Jennings, P. C., R. B. Matthiesen and J. B. Hoerner (1971). "Forced Vibration of a 22-Story Steel Frame Building", Earthquake Engineering Research Laboratory, California Institute of Technology, and Earthquake Engineering and Structures Laboratory, University of California, Los Angeles, Pasadena, California.

Jennings, P. C. (1969). "Spectrum Techniques for Tall Buildings" *Proceedings of the Fourth World Conference on Earthquake Engineering*, Vol. II, Section A-3, pp. 61-74, Santiago, Chile.

McVerry, G. H. (1979). "Frequency Domain Identification of Structural Models from Earthquake Records", Earthquake Engineering Research Laboratory Report 79-02, California Institute of Technology, Pasadena, California.

Newmark, N. M. and E. Rosenblueth (1971). *Fundamentals of Earthquake Engineering*, Prentice-Hall, Englewood Cliffs, New Jersey.

Newmark, N. M. and W. J. Hall (1982). *Earthquake Spectra and Design*, Earthquake Engineering Research Institute, Berkeley, California.

Nielsen, N. N. (1964). " Dynamic Response of Multistory Buildings", Earthquake Engineering Research Laboratory, California Institute of Technology, Pasadena, California.

Porcella, R. L., E. C. Etheredge, R. P. Maley and A. V. Acosta (1994). "Accelerograms Recorded at USGS National Strong-Motion Network Stations During the M_S = 6.6 Northridge, California Earthquake of January 17,1994", Department of the Interior, U. S. Geological Survey, Open File Report 94-141, Menlo Park, California.

Petrovski, J., R. M. Stephen, E. Gartenbaum, and J. G. Bouwkamp (1976). "Dynamic Behavior of a Multistory Triangular-Shaped Building" Earthquake Engineering Research Center Report 76-3, College of Engineering, University of California, Berkeley, California.

Rea, D., J. G. Bouwkamp and R. W. Clough (1966). "The Dynamic Behavior of Steel Frame and Truss Buildings", Structural Engineering Laboratory, College of Engineering, University of California, Berkeley, California.

Rea, D., A. A. Shah and J. G. Bouwkamp (1971). "Dynamic Behavior of a High-Rise Diagonally Braced Steel Building", Earthquake Engineering Research Center Report 71-05, College of Engineering, University of California, Berkeley, California.

Rosenblueth, E. (1951). A Basis for Aseismic Design of Structures, Doctoral thesis, University of Illinois, Urbana, Illinois.

Shakal, A., M. Huang, R. Darragh, T. Cao, R. Sherburne, P. Malhotra, C. Cramer, R. Sydnor, V. Grazier, G. Maldonado, C. Petersen and J. Wampole (1994). "CSMIP Strong-Motion Records from the Northridge, California Earthquake of January 17, 1994" California Department of Conservation, Division of Mines and Geology, Office of Strong Motion Studies, Report OSMS 94-07, Sacramento, California.

Shakal, A. and M. J. Huang (1994). "Recorded Ground and Structure Motions from the 1994 Northridge Earthquake", *Proceedings of the 63rd Annual Convention*, Structural Engineers Association of California, Sacramento, California.

Takeo, M. and H. Kanamori (1996), "Simulation of Long-Period Ground Motion near a Large Earthquake", *Bulletin of the Seismological Society of America*, in press.

Trifunac, M. D. (1970). "Ambient Vibration Test of a Thirty-Nine Story Steel Frame Building", Earthquake Engineering Research Laboratory, Report 70-02, California Institute of Technology, Pasadena, California.

Trifunac, M. D. (1972). "Comparison Between Ambient and Forced Vibration Experiments", *Earthquake Engineering and Structural Dynamics*, Vol. 1, No. 2, Oct.-Dec. 1972, pp. 133-150.

Ward, H. S. and R. Crawford (1966). "Wind-Induced Vibrations and Building Modes", *Bulletin of the Seismological Society of America*, Vol. 56, No. 4, pp. 793-813.

Watanabe, S., Y. Kida and M. Higuchi, "The Vibrational Analysis of a Steel Structure, The Vibrational Test of the Ohbayashi-Gumi Building" (1965). *Proceedings of the Third World Conference on Earthquake Engineering,* Vol. 2, pp. 695-712, Auckland and Wellington, New Zealand.

APPENDICES

APPENDIX I--NOTES ON DATA REDUCTION

Century City Theme Building (Petrovski et. al., 1976)

The second through 42nd floors of this steel-frame building are regularly spaced at intervals of 12' 7". The roof is 36' 2-1/2" above the 42nd floor; a distance 18-1/2" short of three additional floors. The 2nd floor is 36' above the Plaza floor, which in turn is 21' above floor B, and 65' 11" above the lowest floor of parking, level F.

Data from the forced vibration tests were used. In applying the data, the base of the structure, x=0, was assumed to be 5' 11" below level B, giving five 12' 7" levels between this point and the beginning of the regular part of the building at the second floor. The small responses recorded at level B were assumed to apply to the first level, and records at the Plaza floor were assumed to apply at level two. Similarly, roof records were assumed to apply at a level three floors above the 42nd floor, 18-1/2" higher than the actual point of measurement.

The data were then applied to this equivalent 48-story regular structure at the appropriate level. Data were not taken at every floor, and the number of floors between recording sites varied. Mode shape ordinates were linearly interpolated between levels of recordings to provide numerical values of the modes at each of the 48 levels.

Union Bank Building (Trifunac, 1970)

The second through 11th floors of this steel-frame building are spaced at 12' 5" intervals; from the 11th to 38th floor the interval reduces to 12' 1". The 39th floor is 14' 0" above the 38th and the roof is an additional 22' higher than that. The 2nd floor is 21' above the first. Three floors, a street level and two floors of parking, below the first floor total 40' 3/4".

Two data reductions schemes were employed. In the first, the street level was taken as x=0 and the data, which were recorded at every third floor of the structure, were applied at their actual heights. Data were not recorded on the roof and data from the first floor were not used. This approach gives a thirteen level structure, with almost, but not quite, equal

intervals between floors. As a result of this unequal spacing, the 13-level shear beams modes are not orthogonal.

The second approach was the same except that the spacing between the thirteen levels was made equal, preserving the total height. In this case the shear beam modes are orthogonal, but the actual and presumed recording points of the data differ slightly.

The differences in the elements of the B matrix and derived parameters are within one or two units in the second decimal place in most cases, although larger differences are seen in the fifth modes. The values from the second approach, in which the thirteen intervals are equal, are reported in the study.

San Diego Gas and Electric Company (Jennings et al., 1971)

The steel-frame building is regular from floor three through floor 20, with an interstory height of 13' 6". The top two floors, 21 and the roof, have an average spacing of 14' 9". The lower floors of the building, B, A, 1 and 2, have a total height of 58', an average of 14' 6" for each of the four levels. Data were taken at each of the 24 levels: B, A, 1, 2, ..., 21 and the roof.

To apply the data, floors 21 and the roof were assumed to be at the same spacing as the intermediate floors, 13' 6". Similarly the 14' 6" average spacing of the lower four floors was approximated by 13' 6".

Based on the data, the structural layout, and the encasement of the steel columns of the structure in concrete below the first floor level, the building could arguably be considered fixed at the first floor, or alternatively, at a lower floor. Two possibilities were examined: x=0 at the first floor, and x=0 two levels lower, at the B level. The approach with x=0 at the first floor was chosen for presentation.

Parsons (Foutch, 1976)

The building is a 12-story steel-frame tower with a roof; all floors are spaced 14' 0" apart. Data were taken on the first floor, the roof and all intermediate floors except floor 12. In applying the data, the first floor was taken to be x=0 and the response of the 12th floor was approximated

by interpolating between the measurements from the 11th floor and the roof. The resulting regular structure has 12 equal levels.

JPL Building 180 (Nielsen, 1964)

Building 180 on the campus of the Jet Propulsion Laboratory is a 10-story steel-frame structure built on a hillside. It is embedded in such a way that the building is effectively fixed at the second floor. The floors of the building are regularly spaced at intervals of 14'. Data were taken at floors 3 through 10, providing data for a regular structure with eight levels, with x=0 taken at the second level.

Alcoa Building (Rea et. al., 1971)

The Alcoa building is a 27 story, diagonally-braced, steel-frame building. The data were taken at irregular levels in parts of the building and not at all the same locations in the two directions. After examining Burridge and Nalbandian's data reduction and the original reference, it was decided to take the base at mezzanine level (Burridge and Nalbandian's 0.055) and use 15 equally spaced levels. With this approach all data points were used at within $y/l = 0.03$ of their actual positions.

U. C. San Francisco Medical Center-East (Rea et al., 1966)

The building is a 15 story, steel-frame structure. The data used were as presented by Burridge and Nalbandian, with each mode represented by five equally spaced data points. Five modes were recorded in each direction. The data may be too sparse to define the higher modes well and may be affected by the fact that measurements were made at different phases of construction.

The CIL House-Canada (Ward and Crawford, 1966)

This steel-frame building has 34 stories above ground and four below, with a plan of 168' x 112'. Burridge and Nalbandian give the data at 13 almost equally-spaced levels. Data are available from ambient tests for three modes in the transverse direction only. After examining the data in the original reference, it was decided to take $y = 0$ at the level of 0.07 and to use 12 equal levels. The recordings were made at irregular levels in

parts of the building. Comparing y/l for the actual levels with those for 12 equal levels, it was decided to use the data as presented if y/l for the two measures differed by 0.02 or less. For larger differences, data were interpolated to give numbers for the equally-spaced levels. This was done for y/l = 0.42, 0.33, and 0.08.

The Canadian Imperial Bank of Commerce (Ward and Crawford, 1966)

The structure is a 47 story steel-frame building with 44 stories above ground and 3 below. The plan is 140' by 112'. The data are as presented by Burridge and Nalbandian, adapted from the paper by Ward and Crawford. From examination of the data in the original reference it was decided to set y = 0 at the 0.04 level and to use 12 equally spaced levels. This required replacing the bottom two closely spaced data points by a single, interpolated value. Only two transverse mode shapes are reported, obtained from ambient vibrations.

The DIC Building, Tokyo, Japan

The building has 18 stories plus 5 basement floors and a 2-story penthouse. The main tower is 54m x 16.4m in plan. The structure is steel frame above grade and reinforced concrete below. The floors are made of precast, prestressed, single T sections. The data are from Burridge and Nalbandian who give three mode shapes in the NS and EW directions at 18 equally spaced levels (apparently taking the base of the structure at the transition from steel to reinforced concrete). The original reference for the tests was not given.

The Ohbayashi-Gumi Building, Tokyo, Japan (Watanabe et. al., 1965)

The Ohbayashi-Gumi building is a 42-story, braced steel-frame structure. Data are available for five modes in the EW direction. Burridge and Nalbandian present these at five almost equally-spaced levels (1.0, 0.81, 0.61, 0.41, 0.19) corresponding to floors 42, 34, 25, 17, and 8. It was assumed that the data held for five equally-spaced levels: 1.0, 0.80, 0.60, 0.40, and 0.20, and they were analyzed on that basis.

APPENDIX II--TRANSFORMATION MATRICES

IMPERIAL BANK OF CANADA
B MATRIX-TRANSVERSE

0.98	-0.10
0.16	0.94
-0.01	0.31
0.03	0.01
0.05	0.03
0.03	-0.02

CENTURY CITY THEME BUILDING
B MATRIX-EW

0.99	-0.12	-0.01	-0.10	0.10	0.26
0.06	0.95	-0.23	0.09	0.03	0.14
-0.07	0.30	0.88	-0.26	0.33	-0.03
-0.01	0.02	0.42	0.81	0.09	0.25
-0.03	0.00	-0.01	0.49	0.83	-0.10
0.00	-0.03	0.04	0.02	0.39	0.74
-0.01	0.01	-0.03	0.04	-0.07	0.50
-0.01	0.00	-0.01	0.01	0.07	0.00
-0.01	0.00	0.00	0.04	-0.02	-0.03
-0.01	0.02	0.01	0.00	-0.03	0.04
-0.01	0.00	-0.01	-0.04	0.05	0.13
0.00	-0.01	-0.02	0.00	0.07	0.04

CENTURY CITY THEME BUILDING
B MATRIX-NS

0.99	-0.15	-0.04	-0.12	0.08
0.10	0.92	-0.25	0.05	-0.02
-0.11	0.36	0.88	-0.33	0.12
-0.03	-0.01	0.40	0.78	-0.04
0.00	0.01	0.02	0.50	0.83
-0.01	-0.04	0.04	0.07	0.48
-0.01	0.00	-0.04	0.05	0.08
0.00	0.02	0.00	-0.01	0.20
0.00	0.00	0.00	0.02	0.00
0.00	0.02	0.02	0.00	-0.04
0.00	-0.01	-0.02	-0.02	0.03
0.00	0.00	-0.02	0.01	0.08

OHBAYASHI-GUMI BUILDING-JAPAN
B MATRIX-EW

1.00	-0.21	-0.01	-0.03	0.11
0.02	0.95	-0.27	0.08	0.13
0.04	0.24	0.93	0.04	0.22
-0.07	-0.03	0.24	0.99	0.10
0.05	0.03	-0.06	0.10	0.96

UNION BANK BUILDING
B MATRIX-EW

0.99	-0.19	-0.09	-0.01	-0.03
0.11	0.96	-0.21	0.00	-0.09
0.02	0.19	0.93	-0.20	-0.08
0.01	0.06	0.26	0.92	-0.33
0.01	0.03	0.08	0.29	0.87
0.00	0.02	0.00	0.08	0.29
0.00	0.00	0.05	-0.04	0.16
0.01	0.01	0.00	-0.02	0.04
0.02	0.00	0.02	-0.08	0.02
0.01	0.01	0.03	-0.06	0.02

UNION BANK BUILDING
B MATRIX-NS

1.00	-0.13	-0.11	-0.02	-0.03
0.08	0.98	-0.18	-0.05	-0.06
0.03	0.14	0.94	-0.22	-0.16
0.01	0.04	0.25	0.95	-0.28
0.01	0.00	0.05	0.19	0.88
0.01	0.01	0.06	0.10	0.27
0.01	0.01	-0.01	-0.02	0.14
0.01	0.01	0.03	-0.03	0.08
0.01	0.00	0.02	-0.02	0.05
0.01	0.01	-0.01	-0.03	-0.01

THE CIL HOUSE-CANADA
B MATRIX-LONGITUDINAL

0.99	-0.15	-0.01
0.06	0.99	-0.04
0.08	0.00	0.99
0.00	0.05	0.05
0.03	-0.02	0.03
-0.02	0.00	0.07

0.00	-0.02	0.08
0.01	0.01	-0.03

ALCOA BUILDING
B MATRIX-NS

1.00	-0.16
0.05	0.98
0.01	0.06
-0.01	0.05
0.01	0.00
0.00	-0.02

ALCOA BUILDING
B MATRIX-EW

0.98	-0.20
0.20	0.95
0.01	0.23
-0.02	0.00
0.01	0.02
0.00	-0.04

SAN DIEGO GAS AND ELETRIC COMPANY
B MATRIX-EW

1.00	-0.11	-0.04	-0.19	-0.08	0.00
0.09	0.99	-0.05	-0.16	-0.03	-0.06
0.01	0.09	0.99	-0.10	-0.16	0.16
0.00	0.03	0.07	0.95	-0.15	-0.11
0.04	-0.01	0.02	-0.02	0.94	0.24
-0.01	0.01	-0.05	-0.01	0.15	0.84
0.00	0.01	0.03	-0.05	0.11	0.25
0.00	0.02	-0.02	0.05	-0.03	-0.06
0.00	-0.02	0.03	-0.02	0.07	0.12
0.00	0.01	0.00	-0.01	0.06	-0.07
0.00	-0.01	0.01	-0.05	0.05	0.08
0.00	0.00	0.00	0.04	-0.01	-0.05

SAN DIEGO GAS AND ELECTRIC COMPANY
B MATRIX-NS

1.00	-0.20	-0.13	0.20	-0.21	0.40
0.07	0.97	-0.25	0.12	-0.09	0.36
-0.05	0.12	0.95	0.23	-0.05	0.40
-0.01	-0.02	0.12	-0.92	0.11	0.34
0.04	-0.01	-0.04	-0.05	0.94	0.40
-0.02	0.00	-0.02	0.14	-0.01	0.52
0.00	-0.03	0.00	0.04	-0.11	-0.05
-0.01	-0.02	-0.04	0.04	-0.12	0.03
0.01	0.00	-0.03	0.03	-0.02	0.01
-0.01	0.00	0.01	0.00	-0.02	0.05
-0.01	-0.01	0.03	0.00	0.03	0.01
0.01	-0.02	-0.02	-0.04	0.01	0.00

THE DIC BUILDING-JAPAN
B MATRIX-EW

1.00	-0.16	0.09
0.07	0.96	0.04
0.01	0.21	0.98
0.02	0.02	0.11
0.01	0.02	0.07
0.01	0.03	0.02
0.00	0.01	0.03
-0.01	0.01	0.00

THE DIC BUILDING-JAPAN
B MATRIX-NS

1.00	-0.23	-0.08
0.09	0.95	-0.28
-0.01	0.22	0.91
0.01	-0.01	0.27
0.00	0.02	0.05
0.00	-0.01	0.08
-0.01	-0.01	0.03
0.01	0.01	0.01

THE UNIVERSITY OF CALIFORNIA MEDICAL CENTER
B MATRIX-EW

1.00	0.25	0.14	0.22	0.18
0.03	0.97	0.41	0.11	0.24
0.04	0.03	0.90	0.46	0.15
-0.01	0.00	0.04	0.85	0.54
0.02	0.00	-0.05	0.00	0.77

THE UNIVERSITY OF CALIFORNIA MEDICAL CENTER
B MATRIX-NS

0.99	0.24	0.16	0.18	0.15
0.13	0.96	0.37	0.14	0.31
0.09	-0.08	0.91	0.36	0.20
0.04	0.10	0.03	0.90	0.44
0.03	-0.05	0.05	-0.13	0.81

PARSONS BUILDING
B MATRIX-EW

0.99	-0.22	-0.08
0.15	0.94	-0.29
-0.01	0.26	0.88
0.01	0.03	0.35
0.01	0.04	0.05
0.01	0.01	0.07

PARSONS BUILDING
B MATRIX-NS

0.99	-0.21	-0.15
0.17	0.95	-0.08
-0.01	0.23	0.93
0.01	0.03	0.31
0.01	0.02	0.02
0.00	0.02	0.09

JET PROPULSION LABORATORY BUILDING 180
B MATRIX-EW

1.00	0.15	-0.15	0.04
-0.04	-0.99	-0.14	0.27
0.02	-0.05	0.96	0.16
0.00	-0.08	0.05	-0.91
0.01	0.02	0.12	0.01
-0.01	-0.03	0.00	-0.23
0.02	0.02	0.08	0.05
0.00	-0.02	-0.05	-0.10

JET PROPULSION LABORATORY BUILDING 180
B MATRIX-NS

1.00	0.25	-0.22
0.06	-0.96	-0.29
0.03	-0.09	0.91
0.02	-0.05	0.09
0.01	0.01	0.13
0.00	-0.02	0.01
0.00	0.00	0.09
-0.01	-0.04	-0.05